A DSP IMPLEMENTATION OF A SUBSCRIBER LOOP TESTER

A Thesis Submitted
to the College of Graduate Studies and Research
in Partial Fulfillment of the Requirements
for the Degree of Master of Science
in the Department of Electrical Engineering
University of Saskatchewan

by

Ehren Johannes Dirk van Melle

Saskatoon, Saskatchewan, Canada

Spring 2001

PERMISSION TO USE

In presenting this thesis in partial fulfillment of the requirements for a Postgraduate degree from the University of Saskatchewan, it is agreed that the Libraries of this University may make it freely available for inspection. Permission for copying of this thesis in any manner, in whole or in part, for scholarly purposes may be granted by the professors who supervised this thesis work or, in their absence, by the Head of the Department of Electrical Engineering or the Dean of the College of Graduate Studies and Research at the University of Saskatchewan. Any copying, publication, or use of this thesis, or parts thereof, for financial gain without the written permission of the author is strictly prohibited. Proper recognition shall be given to the author and to the University of Saskatchewan in any scholarly use which may be made of any material in this thesis.

Request for permission to copy or to make any other use of material in this thesis in whole or in part should be addressed to:

Head of the Department of Electrical Engineering
57 Campus Drive
University of Saskatchewan
Saskatoon, Saskatchewan, Canada
S7N 5A9

ACKNOWLEDGMENTS

The author would like to acknowledge The Natural Sciences and Engineering Research Council (NSERC) and Telecommunications Research Laboratories (TRLabs) for providing financial support for this research.

Garth Wells and the rest of the staff at TRLabs, Saskatoon, are also thanked for their time, patience, and help during various stages of this project.

Dr. B.L.F. Daku is recognized for his guidance and insight as the author's supervisor for this thesis.

The author would also like to thank his wife for her support and patience over the course of this thesis.

ABSTRACT

The subscriber loop forms the final link between the subscriber and the actual telephone network. The pair of twisted copper wires which form the loop must be well maintained to avoid poor quality service to subscriber or customer. By conducting periodic testing of the subscriber loop, the telephone company can ensure the high standards of service that they desire.

The purpose of this research project is to design a new loop tester based on a digital signal processing (DSP) chip, replacing the old analog-based testers. The DSP chip uses an analog-digital converter (ADC) to take sample measurements of various signals on the subscriber loop and a digital-analog converter (DAC) to output control signals.

Various algorithms are first analyzed and tested to verify their results for the tests required. Next, these algorithms are added to the software running on the DSP chip. The algorithms are then tested versus known input values to qualify the testing procedure and analysis for use on an actual subscriber loop.

Finally, the software is used to provide test results of various fault conditions on a pair of twisted copper wires. The results from these tests show that the DSP-based loop tester can measure varying line resistance and capacitance due to faults present on the subscriber loop, which can lead to accurate fault analysis.

Table of Contents

List of Figures

List of Tables

ABBREVIATIONS

ac	Alternating Current
ADC	Analog to Digital Converter
AWGN	Additive White Gaussian Noise
CO	Central Office
COR	Cutoff Relays
DAC	Digital to Analog Converter
dc	Direct Current
DFT	Discrete Fourier Transform
DM	Daughter Module
DMCB	DM Carrier Board
DSL	Digital Subscriber Line
DSP	Digital Signal Processor
Gbps	Gigabits per Second
Hz	Hertz
I/O	Input/Output
ISR	Interrupt Service Routine
LC	Line Card
LCM	Line Concentrating Module
LEC	Local Exchange Carrier
LIA	Link Interface Adapter
LS	Least Squares
LSI	Loughborough Sound Images Limited
MTA	Metallic Test Access
MTM	Maintenance Trunk Module
MTSO	Mobile Telephone Switching Office
MTU	Metallic Test Unit

nF	Nano-Farads
OC	Optical Carrier
PC	Personal Computer
POTS	Plain Old Telephone Service
RAM	Random Access Memory
Rgnd	Ring to Ground (Ring-Ground)
ROM	Read Only Memory
RLCM	Remote Line Concentrating Module
RMM	Remote Maintenance Module
SRAM	Static RAM
TAC	Test Access Bus
TAR	Test Access Relays
TI	Texas Instruments Incorporated
Tgnd	Tip to Ground (Tip-Ground)
TR	Tip to Ring (Tip-Ring)
V	Volts
VCO	Voltage Controlled Oscillator
V_{ac}	ac Voltage
V_{dc}	dc Voltage
V_{pp}	Voltage peak-to-peak
V_{rms}	RMS Voltage

1. INTRODUCTION

1.1 Background

Telecommunications has become a necessity to modern society. Around the world, wire-line and wireless communications networks provide families with the ability to "keep" in touch and allows businesses to operate in a global economy. The telecommunications network which sprawls around the globe and out into space via satellites, is the backbone of communications in the world today and is commonly taken for granted due to it's commonplace.

Disruptions in this global network can have effects ranging from interrupting world trade and business decisions to isolating a family member from loved ones. Without a responsive, realiable network to transfer the voice or data being communicated, modern society would not exist as it does today. For this reason, communications networks and equipment are designed, built, and tested to withstand various failures and conditions. This is done in many ways, for example, by choosing optimum components, building redundancy, error detection and correction into systems, and maintaining a highly skilled technical support staff to analyze and fix problems.

A large portion of the communications network in developed countries is in the form of copper wire, often buried underground, and only maintainable through manual servicing. The copper wire is the link between a common subscriber, such as a family household, and the telecommunications network. Without a strong, realiable connection into the system, the entire network becomes useless to the common subscriber. Therefore, this part of the network must be maintained to a high standard, since techniques such as redundancy, which can be used to overcome issues in other parts of the network, cannot practically be applied here.

To help maintain the copper wire connecting the subscriber, special equipment and tests have been implemented to detect potential issues and help solve immediate problems. Preliminary testing is used to determine that problems may have arisen and further testing is necessary to determine a more precise analysis. Subsequently, intermediate test results can give service personnel information leading to possible causes and locations of problems. More advanced tests can be later be used near the location of a possible fault to exactly pin-point the location and cause. With the help of the testing equipment, the service provider is able to maintain the expected high quality of service to the individual subscriber.

1.1.1 Motivation for Research

The motivation for the work described in this thesis is to improve upon the current testing equipment and techniques which are used to test the copper wire connecting the subscriber to the rest of the telecommunications network. This connection is commonly called the subscriber loop. Current equipment can be traced back to designs from the 1970's, which results in bulky equipment and slow, limited tests, relative to today's standards. By utilizing modern day equipment and techniques, it is desired to replicate current tests and allow easy upgradability for more tests to further analyze the capability and efficiency of the copper wire.

1.1.2 Prior Research

Much of the recent work done on measurements of the subscriber loop has been for the purpose of determining the potential of the cable to carry high-speed data. A common example would be a digital subscriber line (DSL) connection. Other prior art, which focused on measuring basic loop parameters, was based on a popular technique involving charge integration of the decaying line voltage [1]. Much of this work primarily concentrated on improving the measurement techniques, often by either speeding up the process [2], making more accurate measurements [3], or expanding the testing capabilities [4] [5]. Newer techniques have also been developed for making some of the subscriber loop parameter measurements; one such development utilizing

a multi-frequency test signal to determine the line impedance [6].

1.2 Purpose of Thesis

The purpose of this thesis is to show that the implementation of an intermediate subscriber loop tester on a digital signal processing (DSP) chip is an accurate, efficient, and easily upgradable approach. In doing this, it is also necessary to stress the importance of the subscriber loop and the problems that can occur on the loop which require testing and repair. This also prompts a brief theoretical analysis of the loop.

It is also important in this thesis to prove the data analysis techniques which are implemented on the DSP-based tester. The algorithms which are used in this thesis may also be applied to similar uses in other projects doing sampled data analysis.

Finally, it is also desired that this thesis provide the reader with some insight into the powerful domain of digital signal processing, which provides a simple, yet strong backbone to this entire project.

1.3 Thesis Organization

This thesis will be divided into 6 chapters. Chapter 2 provides detailed background information to the reader and also describes the problem that is being addressed. Chapter 3 delves into the system design used for the project, describing the desired measurement procedure. Measurement algorithms and implementation details can be found in Chapter 4, while Chapter 5 shows the results from the actual measurements. Finally, Chapter 6 will conclude the thesis.

2. SUBSCRIBER LOOPS AND PRESENT MEASUREMENTS

This chapter will provide an introduction to the subscriber loop and it's place in the telephone network. A theoretical description of the loop will be covered, as well as a discussion of problems that occur on the loop and how they are currently being measured.

2.1 The Subscriber Loop

2.1.1 Network Overview

The telephone network is a necessary tool which is taken for granted in our everyday lives. Almost every household in North America has a telephone connection, while most businesses could not even function without telephones. Consisting of copper wire, fibre optic cable, and wireless transmission, the telephone network forms a seemless, global path for communications. This broad network is capable of handling voice, facsimile, internet, and data transmission.

The telephone network has been designed in a combination of hierarchical and mesh structure. The structure is based on the need to make connections over increasing distances, and is ultimately determined by switching centers. A switching center is a hub that receives requests for connections on some lines and then switches the calls to the desired destination on other lines. In the case of a local call, the connection can be made directly through one central office (CO)[1], the name of the lowest level and most abundant type of switching center. In the case of a long distance or toll connection, the central office switches the connection to a higher level switch,

[1]The central office is also known as a Class 5 or Local switching center.

which can reach further destinations and begin billing once the connection is complete. Connections requiring longer distance may also have to be switched through a higher level switching center and so on, as seen in Figure 2.1. The North American public network architecture has a total of five switching levels in this manner [7]. As

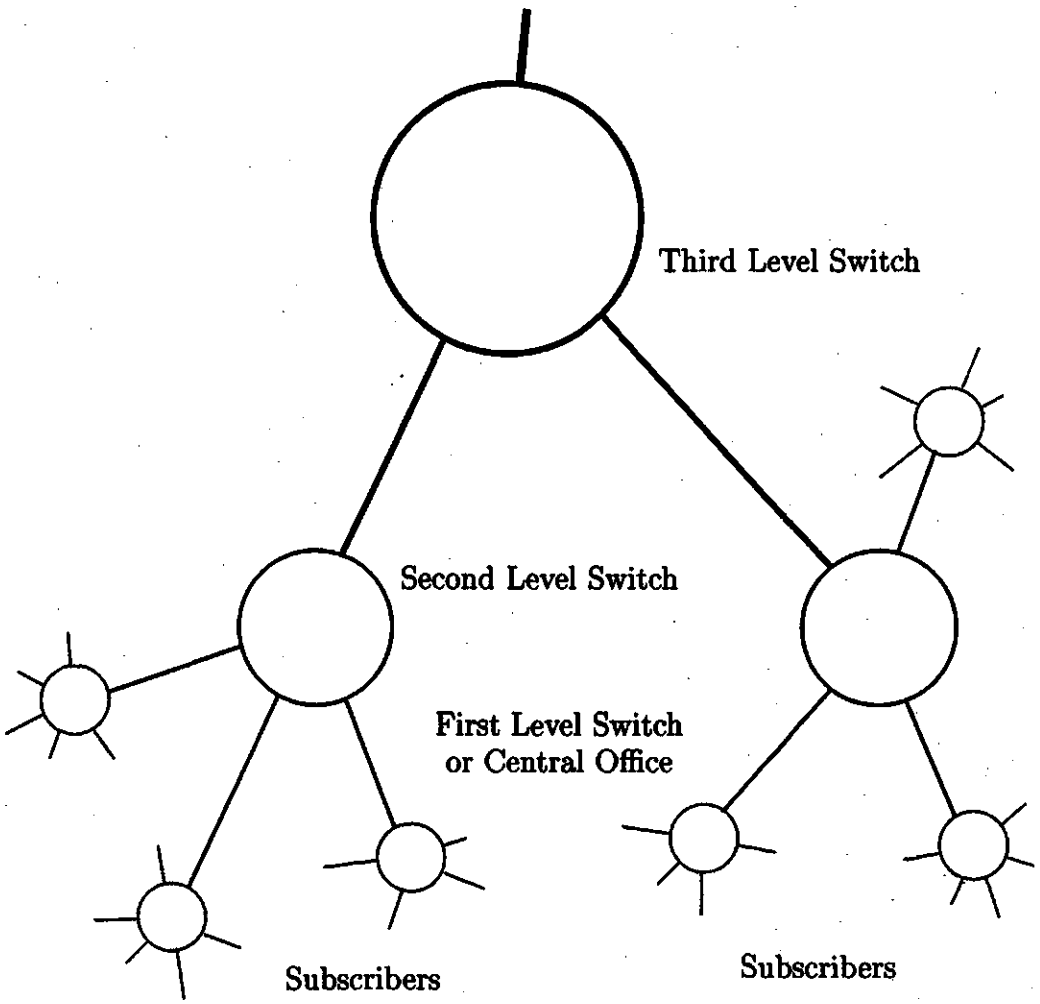

Figure 2.1 Hierarchical Telephone Network

the connections advance to each higher level, the calls are multiplexed together on a higher speed transmission line. Once the calls reach the higher levels, the bit rate can be well into the gigabits per second[2] (Gbps), as the number of supported calls on the line increases.

[2]Optical Carrier (OC)-24 = 1.24416 Gbps, OC-36 = 1.86624 Gbps, OC-48 = 2.48832 Gbps [7]

The telephone network also includes wireless mobile customers in it's scheme. Mobile calls are transmitted from towers to a mobile telephone switching office (MTSO). From here the calls can then be directed to another nearby mobile customer, or can be switched over to a central office to reach a distant destination.

The plain old telephone service (POTS), is the fixed, voice transmission component of the network and is the primary concern of local exchange carriers (LECs). Most problems which occur in the telephone network can be found somewhere between the subscriber and the central office. Following the connection from the subscriber's telephone, the trasmission path consists of a pair of twisted copper wires, typically ending at a line card (LC) housed in a line concentrating module (LCM) at the central office [8]. In many areas, a remote LCM (RLCM) will actually collect the twisted pairs before the central office, so that many signals can be passed through the line cards and multiplexed together for more efficient transmission to the central office. In either case, the link formed by the twisted pair from the subscriber to the line card, is called the *subscriber loop*.

The subscriber loop carries the analog signal from the subscriber's telephone to the subscriber loop interface in the central office or remote center. The subscriber loop interface provides seven main functions to the loop, as follows:

1. *Battery*: Typically -48 Volts (V) is applied to the loop to enable dc signalling.
2. *Overvoltage Protection*: Basic protection of equipment and people from lightening strikes and other high voltage situations.
3. *Ringing*: The application of a 20 Hz, 86 Volts rms (V_{rms}), 2 seconds on, 4 seconds off.
4. *Supervision*: Detection of off-hook or on-hook by flow of dc current.
5. *Coding*: Analog-digital and digital-analog encoding/decoding of signals.
6. *Hybrid*: Conversion from two-wire to four-wire transmission.

7. *Test*: Access to line test towards subscriber or back to switch.

These seven components are referred to as *BORSCHT*[3] and provide the necessary functions at the end of the subscriber loop. The portion of the interface which will be examined in more detail and is the focus of this project is the testing function.

2.1.2 Theoretical Description

The subscriber loop, consisting of a twisted pair of copper wires, can be viewed as a transmission line for theoretical purposes. To ease analysis of relatively short transmission lines, parameters, such as capacitance, can be lumped together as long as the wavelength is somewhat greater than the length of the line [9]. By examining a typical copper pair, we can see that this condition can be met. For example, by choosing a 1000 Hz signal on a 26 gauge pair, the wavelength of the signal is calculated to be approximately 30 km. Since 95% of subscriber loops are less than 5 km long and voice signals are limited to an upper frequency of approximately $\sim$ 3.4 kHz, it is obvious that the length of a typical telelphone line is a fraction of the wavelength of the signal they normally carry. Although the ratio of wavelength to line length is not very large (approximately 6:1 for a 1000 Hz signal on a relatively long line), the lumped model will be used for analysis throughout the remainder of this thesis.

Once it has been decided to lump the parameters together, an electrical equivalent circuit can be formed to represent the line. In the case of making measurements on the loop, the circuit [4] must also include foreign noise sources, as can be seen in Figure 2.2, where tip and ring represent the pair of copper wires forming the loop. C_{ta} and C_{ra} represent the capacitance between the tip wire and the ac interference source and the ring wire and the ac interference source, respectively. Similarly, R_{td} and R_{rd} represent the resistance between the tip wire and the dc interference source and the ring wire and the dc interference source respectively. Also, C_{tr} and R_{tr} represent the

[3]BORSCHT is an acronym for the 7 functions.

[4]This circuit is similar to the one used by engineers at Nortel Networks Corp. when one of the currently used tests units was developed in the 1970's. See Section 2.2 for more details.

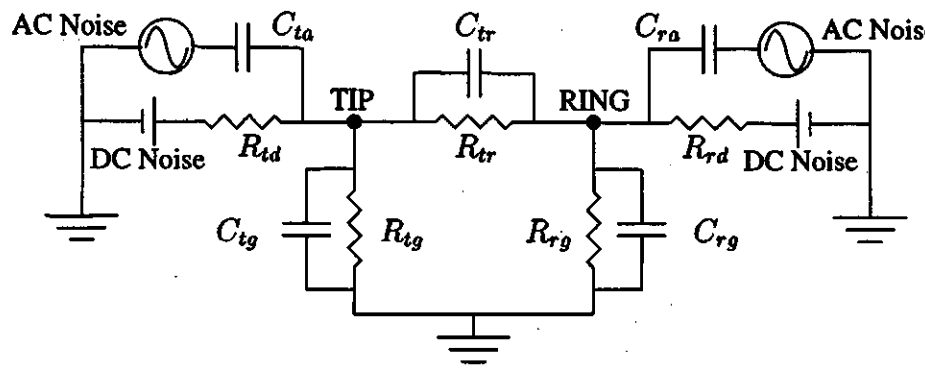

Figure 2.2 Subscriber Loop Equivalent Circuit

resistance and capacitance between the tip and ring wires themselves. Finally, the resistance and capacitance between each of the wires and ground are given by C_{tg}, R_{tg}, C_{rg}, and R_{rg}. The ac noise sources are capacitively coupled to the pair while the dc noise is theoretically connected through a large resistance. This is the circuit used when measuring foreign voltages on the line, but the circuit can be simplified for determining the resistance and capacitance parameters of the system. For parameter measuring purposes, R_{td}, R_{rd}, C_{ta}, and C_{ra} are lumped together with the other tip-ground and ring-ground components. This results in a simplified circuit as far as the number of parameters left to measure, but the results may need to be more closely analyzed to determine just what a change in one parameter may mean for the entire system. For example, if R_{rg} is measured to be relatively small, does it mean that there is a short-circuit to ground or a short-circuit to a dc noise source? When it comes to finding the fault in the line, it does not matter, since other measurements can be used in conjunction to determine exactly what the situation is. The new simplified circuit is shown in Figure 2.3.

The components shown in Figure 2.3 are the resistance and capacitance between tip-ground, ring-ground, and tip-ring. The resistances to ground are typically very large values (> 5 MΩ) [10], indicating that the line is well isolated from ground and is not experiencing losses through a fault to ground. The capacitances to ground are normally quite small and do not help in analyzing the line. The resistance from tip to ring varies with loop length, since the resistance along the loop increases with length.

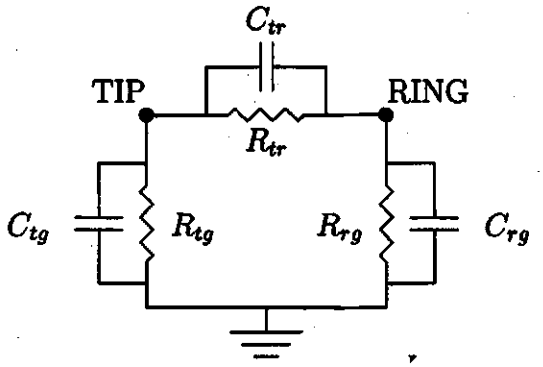

Figure 2.3 Subscriber Loop Simplified Circuit

This is only useful in rare circumstances, since the subscriber's telephone at the far end of the loop has a typical on-hook resistance well into the MΩ, causing the loop resistance to become insignificant. The capacitance from the tip to ring, on the other hand, offers more information about the line. This measurement may range anywhere from 1 - 350 nF and under normal conditions can be used to determine the length of the loop. This is done by multiplying the measured capacitance, from either tip to ground or ring to ground, by a known factor based on the gauge of the wire.

2.1.3 Problems on the Subscriber Loop

A large number of the problems which occur on a subscriber's telephone line are caused by a problem on the wire pair. This is often referred to as a line fault. The purpose of testing the subscriber loop is to determine where a line fault is occuring or may possibly occur. The primary consideration when investigating a line fault is to isolate the problem to one of the following items that make up a line:

- line card
- line concentrating device
- subscriber loop pair
- telephone equipment

The problems can often be found on the subscriber loop, which is susceptible to many conditions. The pairs of wires, running throughout entire cities, are prone to problems due to excess noise, open circuits, and various short circuits that may occur [1]. To ensure quality service to the customer, the loops are tested on installation and routinely throughout their service life. Testing can also be done following a customer complaint to determine if a fault is the source of the problem.

Typical line faults include excess electrical noise from other lines running nearby or overhead, short circuits between the 2-wire pair or between one or both of the wires to ground or to a nearby telephone line, and open circuits on either one or both of the wires. The following descriptions discuss each of these issues in more detail.

Most of the excess noise which can cause problems on the loop is a result of 60 Hz (and harmonics) signals present on the line [11]. These signals are capacitively coupled or could possibly be in direct contact with the pair (if C_{ta} or C_{ra} was zero), as shown in Figure 2.2. This is possible due to the fact that many power lines run parallel to bundles of copper pairs, both underground and on overhead lines. The 120 V_{rms}, 60 Hz signals are large enough to easily couple large components on the loop. Although standards have been set to keep interference from power lines to a minimum, it is still a common occurence.

Other noise on the lines can appear as dc noise which is coupled from other lines in the same bundle. Higher frequency noise, such as interference from radio stations, can also appear on the loop[5], but this does not hinder normal voice traffic. This is due to band limiting filters which limit the high frequency noise at the central office and a low pass frequency response of the circuit in the subscriber's telephone. The problems caused by excess line noise include false operation of circuits and unsatisfactory signal-noise ratio (SNR) at the subscriber's set.

Short circuits on the loop are often a problem and can sometimes be very difficult to diagnose. A short on the pair can occur between tip-ring or between either or both

[5]Above ground open wire is very susceptible to radio wave interference.

lines to ground. The cause of a short can be due to deterioration of insulation, damage of insulation from rodents, damage of insulation from humans, and other factors which could cause one of the wires to make contact elsewhere. These faults become hard to diagnose when the fault becomes intermittent. This occurs if the fault is normally of high resistance, therefore not significantly affecting service. When water is present though, the water creates a low resistance path which can then cause problems on the line. For this reason, some faults can only be found in wet conditions such as rain. Shorts on the line can ultimately cause false operation of the circuits which monitor the line, poor connections due to unbalanced lines, and lead to possible equipment damage.

The final common fault which can occur is an open circuit, on either one or both wires of the pair. Open circuits are often a man-made situation, although natural factors could cause an open circuit. If care is not taken when digging underground, a bundle of twisted pairs may be cut, causing loss of service to a large number of subscribers. Although this is a major occurence, it is often easy to diagnose and locate the fault based on customer complaints and knowledge of crews working in the area.

2.2 Current Measurement Setup

Testing of the subscriber loop is conducted from the central office or remote switching center, depending on the location of the line card. The tests are conducted by a metallic test unit (MTU) which is located in the maintenance trunk module (MTM), if at the central office, or in the remote maintenance module (RMM) if at a remote office. A metallic test access (MTA) provides access to the subscriber loop via the test access bus (TAC), while cutoff relays (COR) on the line card isolate the loop from the LCM and the rest of the telephone network, and test access relays (TAR) connect the line to the TAC, as shown in Figure 2.4 [8].

The MTU consists of an analog board (NT4X98 / NT2X10BA) and a controller board (NT4X97 / NT2X11BA) [12], which were designed and manufactured by Nor-

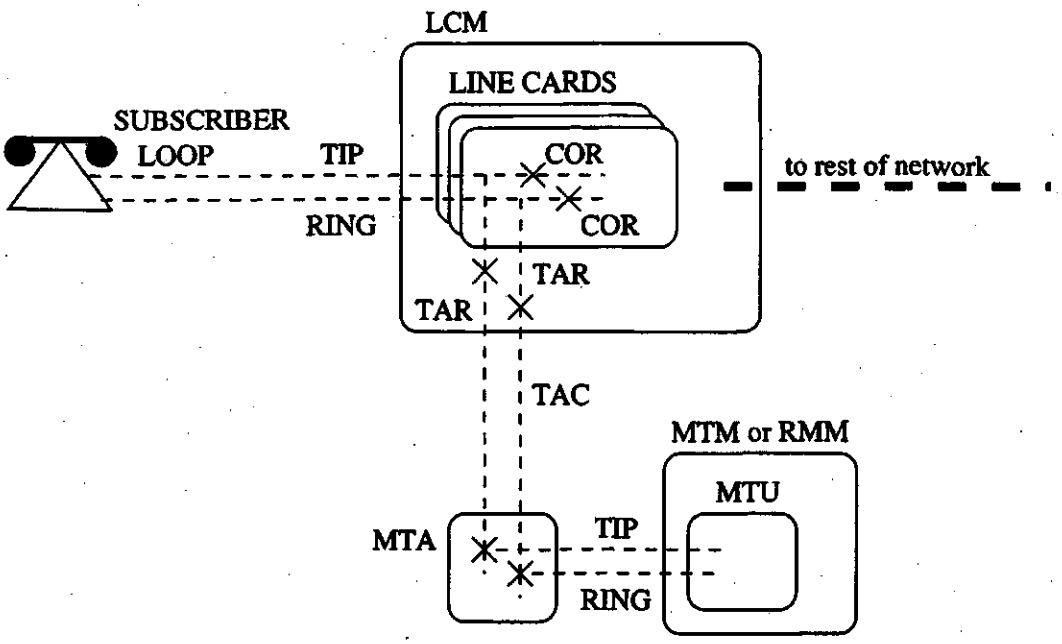

Figure 2.4 Block Diagram of Current Test Setup

tel Networks Corp.. The analog board is home to the measurement test head, a switching mode power module, relay arrays, opto-coupler arrays, voltage-controlled oscillators (VCO), differential amplifiers, ac/dc converters, resistance terminations, calibration reference, and other analog components. The controller board contains the microprocessor, ROM, RAM, and other digital devices. Communications between the two boards takes place via a dedicated 22 conductor bus, called the MTU bus. The two boards occupy adjacent slots in the MTM or RMM, with each set providing two independent test units.

The software of the MTU runs on an 8085 microprocessor based multitasking, real time operating system. A Transient Charge Measurement algorithm [1] is used to measure all of the subscriber loop parameters, as listed below:

- dc Voltage (tip-ground, ring-ground, tip-ring)
- ac Voltage (tip-ground, ring-ground, tip-ring)
- Resistance (tip-ground, ring-ground, tip-ring)

- Capacitance (tip-ground, ring-ground, tip-ring)
- Frequency (of ac Voltages)

For each measurement state, stimulus voltages in the range of $\pm$ 100 V_{dc} are applied by digital to analog converters (DAC) to the test head through output resistors. The stimulus current is then continuously monitored and converted into frequencies of digital pulses, which are counted by the MTU controller card. There the counts are processed for analog to digital conversion and charge integration. Frequencies of the external ac signals are detected by zero-crossing detectors and sent back to the controller for generating synchronization signals. The MTU can communicate the final measurements back to the switch through an interface circuit in the MTM or RMM. A simplified diagram of the NT4X98 functional blocks is shown in Figure 2.5. The measurement specifications for a line test unit (LTU), a card providing the basic functions of the MTU, are shown in Table 2.1.

The MTU includes additional features such as electronic business set testing capability and high frequency pulse measurement, although these are not measurements of the physical loop parameters.

When subscriber loop tests are conducted, a *PASS* or *FAIL* is reported when the measured values are compared with established limits [8]. Table 2.2 lists the threshold values which must be met on the subscriber loop.

Looking closely at the values in Table 2.2, it is obvious that large voltages may sometimes appear between each line to ground and can still be within allowable limits. However, if a large voltage appears on only one line, although it may be within the line-ground limits, this could cause the tip-ring voltage measurement to be exceeded. Therefore, if a large voltage is common-mode, or common to both tip and ring, then the tip-ring voltage will be small, although the tip-ground and ring-ground voltages may be large - this could still result in a *PASS*. A large voltage which appears on only one of the lines, would result in a differential voltage between tip and ring, which could result in a *FAIL*. This indicates that a well balanced pair, which deters noise,

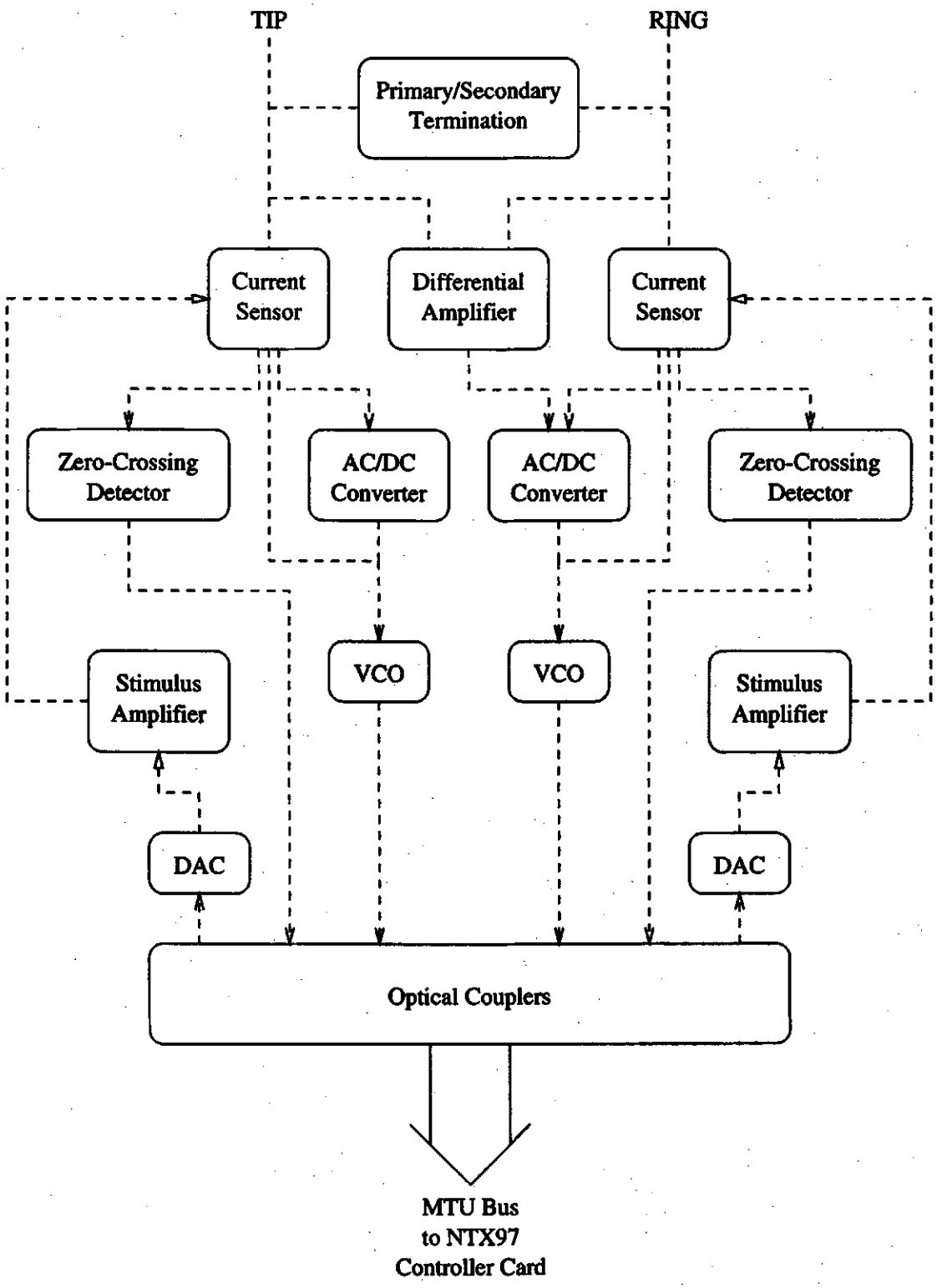

Figure 2.5 NT4X98 Functional Block Diagram

Table 2.1 LTU Measurements Specifications

Measurement	Range	Resolution	Accuracy
Resistance	10 to 99 Ω	1 Ω	±8%
	100 to 999 Ω	1 Ω	±4%
	1 to 9.99 kΩ	10 Ω	±4%
	10 to 99.9 kΩ	100 Ω	±4%
	100 to 999 kΩ	1 kΩ	±10%
Capacitance	0.01 to 0.99 μF	0.01 μF	±10%
	1.00 to 5.00 μF	0.01 μF	±10%
dc Voltage	−150 to +150 V	1 V	±1 V or 5%
ac Voltage	0 to 150 V_{rms}	1 V	±1 V or 5%
Frequency	0 to 255 Hz	±1 Hz	±1 Hz
** Note: Resistance > 999 kΩ appear as 999 kΩ*			

Table 2.2 Measurement Threshold Values

	Tip to Ring		Tip to Ground		Ring to Ground	
Parameter	**Min**	**Max**	**Min**	**Max**	**Min**	**Max**
Volts dc	-10	+10	-60	+60	-60	+60
Volts ac (rms)	0	10	0	120	0	120
RES (kΩ)	800	∞	800	∞	800	∞
CAP (μF)	0	4	0	4	0	4

is much more likely to *PASS* the allowable thresholds, even in the presence of excess induced voltage.

2.3 Summary

The subscriber loop is an important part of the entire telephone network and must be treated as such. Frequent testing is an important tool for maintaining service. By examining the equivalent circuit for a subscriber loop, appropriate measurements can be made to find the desired parameters and identify faults.

3. PROPOSED MEASUREMENT SYSTEM

This chapter provides an overview of the new, DSP-based test system that was designed for this project and used to conduct tests in the lab. This includes a detailed description of the hardware that was used, including the DSP chip itself. An overview of the software system is also included to give an entire picture of the measurement system.

3.1 Hardware Description

To understand how the hardware works, it is important to first understand the layout of the fundamental pieces and how they fit together. Figure 3.1 shows a simple view of the entire system. The DSP chip resides on a card that plugs into a personal

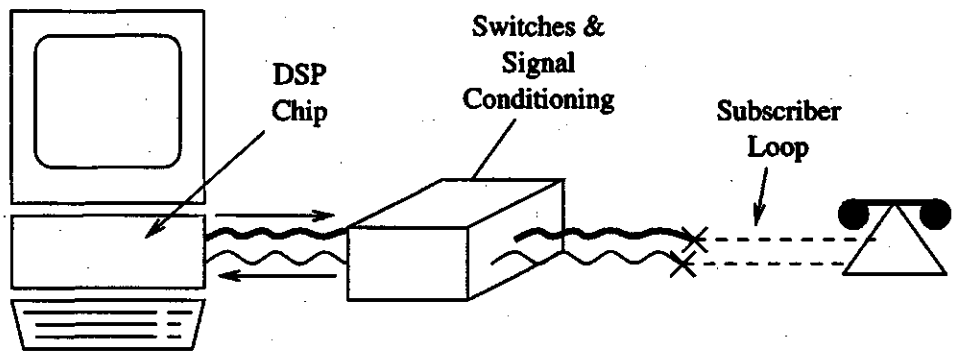

Figure 3.1 Hardware Physical Layout

computer (PC). The card is then connected to the subscriber loop through a specially designed interface. Output signals from the card control the hardware interface components, while input lines are used to measure the desired signals. Figure 3.2 shows an architectural block diagram of the same hardware components. The following subsections describe the blocks shown in this figure.

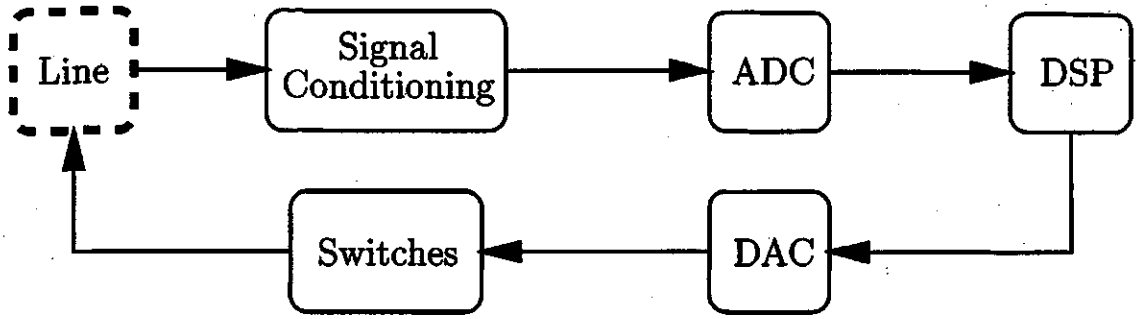

Figure 3.2 Hardware Block Diagram

3.1.1 The DSP

The DSP chip that was used for this project is Texas Instruments' (TI's) TMS320C40. The chip used is actually one of four which ultimately reside on a Quad C40 Processor Board (QPC/C40B) from Loughborough Sound Images'(LSI) [13]. The QPC/C40B is home to four MDC40S modules (also supplied by LSI) which are designed to meet TI's TMS320C4x Module Specification (TIM-40) (see Figure 3.3). Each MDC40S module consists of a TI TMS320C40 processor with three banks of 128K x 32 bit zero wait state static RAM (SRAM) [14].

The TMS320C40 processor is the first of TI's TMS320C4x generation floating-point processors [15]. It has two external 32 bit address and data buses and a total memory address space of 4G x 32 bit. Operating at a clock rate of 40 MHz it can achieve a performance of 20 Million Instructions Per Second (MIPS). This rate also allows a peak arithmetic performance of 220 Million Operations Per Second (MOPS). The processor also has six 8 bit communication ports which make it useful in parallel systems, which is the focus behind including four MDC40S modules on the QPC/C40B. Although the four processors are available, only one has been used for this project.

Memory for the processor consists of two blocks of internal zero wait state RAM and the three blocks of on-module external zero wait state SRAM mentioned earlier. 2K x 32 bits of contiguous memory can be divided up accordingly between the two blocks of internal RAM, while the external SRAM is made up of two blocks of 128K

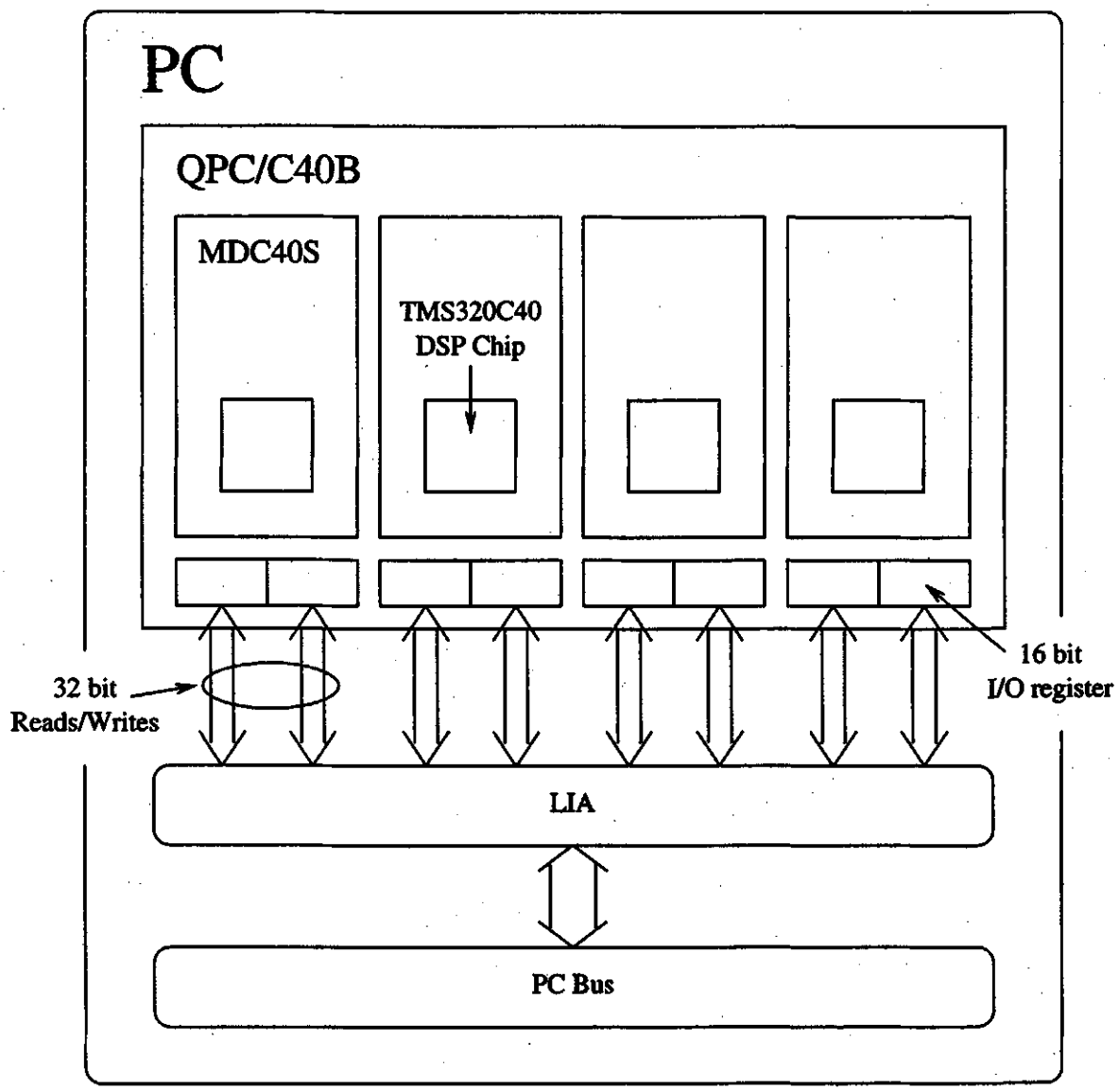

Figure 3.3 DSP Chip and Surrounding Components

x 32 bit in local memory and one block of 128K x 32 bit in global memory. The zero wait state allows memory access times of 26 ns at 40 MHz. These memory banks can be specified to allocate certain sections of the code into each memory block.

Direct communication between the PC and each of the MDC40S modules takes place using the on-board Link Interface Adapter (LIA) via the PC bus. The LIA is accessed through one of the six communication ports and consists of two 16 bit input/output (I/O) registers in the PC I/O map, allowing 32 bit reads and writes.

Software written on the PC was used to open the desired processor and download the DSP code. Communication between the PC and DSP then took place using library functions. This allowed passing of captured and calculated data, as well as simple hand-shaking to monitor progress.

When data is to be written from the PC to the DSP, the PC function polls the LIA data transmit flag before writing any data to the LIA. This ensures that no data will be lost by writing the data before the DSP is ready to receive. At the same time, the DSP will wait and read the data from the communication port when it is available. Similarily, when the DSP sends data to the PC, the data is written to the communication port and the PC will only begin reading the data once the LIA data receive flag is set.

A software debugger was also supplied with TI's DSP chip, which was used to help debug problems in the DSP [16] [17].

3.1.2 The ADC/DAC

The ADC/DAC used in conjunction with the DSP board is the Burr-Brown analog Daughter Module (DM), also from LSI [18]. The Burr-Brown DM is a 16 bit dual-channel module with a maximum sample rate of 200 kHz for the ADC and a maximum reconstruction rate of 500 kHz for the DAC. Both analog inputs have a maximum voltage span of +/-3 V, allowing a resolution of 0.092 mV, with typically a 20 kOhm input impedance in each path. The analog outputs also have a voltage span of +/-3

V and are capable of driving 600 Ohm loads. The DM is also equiped with low-pass filters which can be enabled or disabled on both the input and output. The cut-off frequency may be altered by interchanging resistor packs. They are currently set for 18.3 kHz cutoff, but have been disabled since they are not necessary for the tests being conducted. The input low-pass filters can be used to limit noise and provide anti-aliasing protection. The output filters can be used to smooth the stepped DAC output signals.

Sample rate generation is software programmable up to 200 kHz as already stated. The programmed value for a specific sampling rate is calculated with a simple formula as shown:

$$h = 1 - \frac{F_{CLK}}{F_S}, \tag{3.1}$$

where h = the value to be programmed in the sample rate register,

F_{CLK} = frequency of the prescaled selected clock,

and F_S = desired sampling rate.

For the sample rates used in this project, a selected clock of 12.288 MHz was used with a prescale factor of 4. This gave $F_{CLK} = 3.072$ MHz. For example, if the desired sampling rate is 1024 Hz, then

$$\begin{aligned} h &= 1 - \frac{3.072 \times 10^6}{1024}, \\ &= -2999. \end{aligned}$$

Before this number can then be written in the correct register, it must be converted to hexidecimal from decimal form as follows:

$$\begin{aligned} 2999_{dec} &= 0000101110110111_{bin}, \\ -2999_{dec} &= 1111010001001000_{bin}, \\ &= F448_{hex}. \end{aligned}$$

Therefore, $F448_{hex}$ would be written in the register to set the 1024 Hz sampling rate.

The interface between the DM's and the DSP is provided by the PC Daughter Module Carrier Board (PC/DMCB) [19]. The carrier board holds two DM's and connects to the DSP board via LSI's DSPLINK interface, a high speed, bi-directional bus. With two DM's, there is then a total of four input channels and four output channels which can be used. The DSPLINK is then memory mapped into the DSP memory for accessing module memory.

When a sample is taken and the input sampling buffer is full, an interrupt is generated to the DSP. The input buffer is then read and interrupts are cleared. The DSP can then store the sampled data and wait for the next sample to be taken. The same method works when reconstucting data. A sample is written to the output buffer where it is then reconstructed. At the time the output buffer is read, an interrupt is generated which signals the DSP to write the next sample into the output register.

3.1.3 Signal Conditioning & Switches

As mentioned earlier, the external hardware used for the DSP Loop Tester functions as an interface between the ADC/DAC and the loop itself. The input to the ADC had to be isolated from the line so that it's 20 kOhm input resistance did not load down the line. This was done with a simple op-amp voltage-follower[1]. This also protected the ADC from large input signals, as the op-amp will be destroyed before the large signals can reach the ADC.

The input to the voltage-follower was also modified using a simple, resistor based voltage divider. This permitted the input of relatively large signals to the ADC and allowed the original level to be known by scaling up the voltage based on the known resistance used in the network. The voltage divider could also be varied to different scaling factors, allowing measurement of various signal sizes.

Three signals from the DAC were actually used as switches for other hardware. One such output controlled a series of three power field-effect transistors (FETs).

[1]See Appendix A for a detailed schematic of this circuit.

These FETs supply a known voltage source to the line when line resistance and capacitance are to be measured and also provide protection to the DAC from dangerously high line voltages.

The other two signals are control lines for an analog multiplexer which controls which element will be connected to the line throughout the testing. The current element options include known resistances, a short circuit to supply, and an open circuit. Expanding on a piece of Figure 3.1, Figure 3.4 shows where these elements are switched on/off the line being sampled.

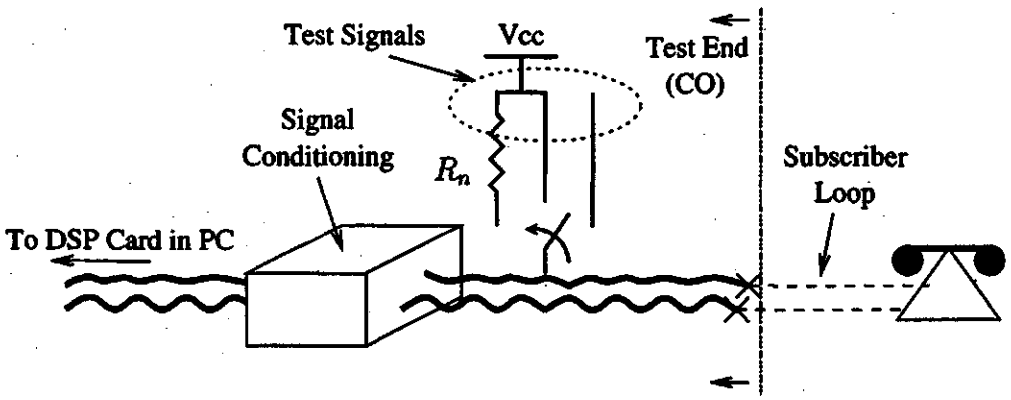

Figure 3.4 Test Signals Applied to the Subscriber Loop

3.2 Software Blocks

The software for this project includes code written for the DSP chip and the PC where the DSP card was installed. Figure 3.5 shows a simple block diagram of the software and the interaction between both platforms.

Upon execution of the software on the PC, the PC loads the DSP code from the appropriate files into memory on the MDC40S module. Once completed, the PC then halts while waiting for the DSP to begin relaying results. As the DSP continues to upload the results for the different stages of the testing, the PC software simply stores the data, outputs the important values to the monitor, and waits for the next set of

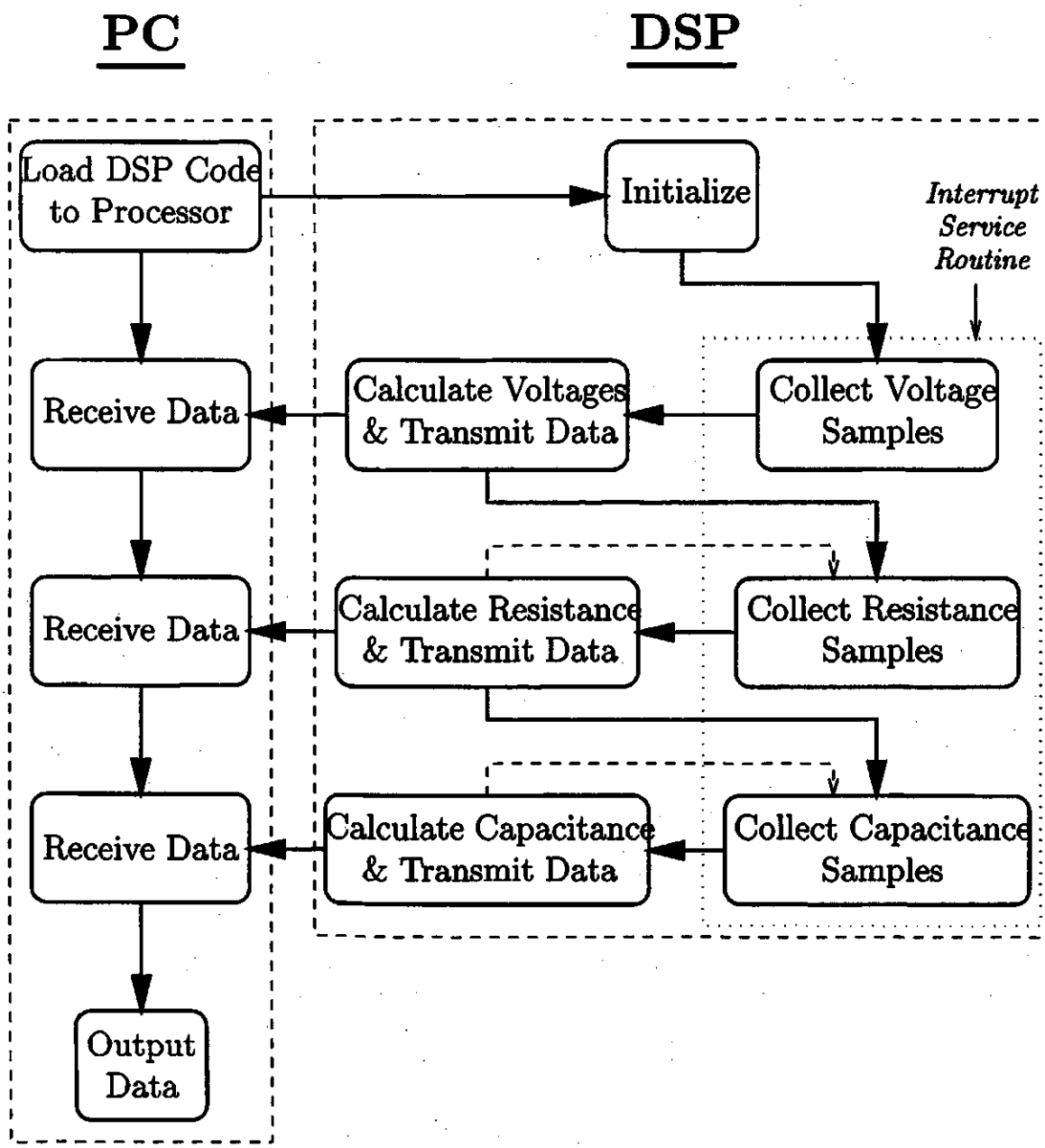

Figure 3.5 Software Block Diagram

data. Once the final set of results has been returned to the PC, the software dumps all of the values to files for subsequent investigation.

While the PC software is used basically as an interface between the user and the DSP, the DSP software is responsible for controlling the hardware, making the measurements, and calculating the desired parameters. Upon initialization from the PC, the DSP software begins by setting up the necessary parameters and installing the interrupt service routine (ISR), which is used throughout the test process to gather the data samples used for the various measurements. The main process then begins by stepping through various stages of the code.

The first step is the collection of voltage samples which are then used to determine the various parameters of the line voltage. This data is then passed to the PC, which has been waiting since loading the DSP software. Upon acceptance from the PC, the DSP continues with gathering the resistance samples. Final resistance values are then calculated and passed to the PC, similar to the initial exchange for voltage measurements. Finally, the ISR reads the samples used for the capacitance calculation. The DSP makes the final measurement calculations, passes the data to the PC, and is then finished operation until the software is re-run.

Chapter 4 will discuss the details of the DSP software described above and shown in Figure 3.5.

3.2.1 Data Transfer and Output

Data transfer takes place following each measurement. Each set of data collected for analysis is also transfered to the PC so that it can be written to a file for further analysis using MATLAB ®. The final results of the measurements are converted from floating point values to integers so that they can be transmitted to the PC. Due to this conversion, some of the significant figures can be dropped; therefore, scaling factors are used to save as many significant figures as possible. The final values are then output to the monitor where they can be viewed by the user. The data is also be written to a file and could be transfered directly to another computer if network

facilities exist.

3.3 Summary

Chapter 3 presented a description of the measurement system that was designed and tested for this project. The hardware components provided a complex, yet very powerful backbone for the DSP software. This allowed the software design to focus on the primary goal, measurement/testing of the subscriber loop. More details about the algorithms implemented in the DSP software are described in Chapter 4.

4. MEASUREMENT ALGORITHMS

The system software outlined in Section 3.2 implemented multiple algorithms for retrieving and analyzing the data necessary for making accurate estimates of the subscriber loop parameters. Most of these algorithms also required testing and verification before formal test results could be gathered. This chapter describes the algorithms which were used in the DSP based tester and in post-processing data analysis.

4.1 Voltage Measurements

The line voltage is an important parameter to measure as it can expose major problems, which canresult in dangerous conditions. Shorts circuits between the twisted pair and 60 Hz power lines can cause very large signals to be present on the line. When the loop is tested and noise signals detected, tests can either be halted to prevent equipment damage, or in the case of smaller signals, can continue in hopes of finding more information.

The voltage measurement is a simple procedure, sampling the signal through the voltage-follower at a rate of 1024 samples per second and collecting a total of 2048 quantized samples (2 seconds of data). The samples are then converted to floating-point voltage levels on the DSP chip so the signal can be analyzed. The dc level of the signal is found by averaging all samples taken. Maximum and minimum levels of the signal are also stored during the sampling process. In the case of a single sine wave being presented to the ADC, frequency f can be estimated from the zero-crossings of the measured values using:

$$f = \frac{(X-1)f_s}{2n}, \tag{4.1}$$

where X = the integer number of crossings found,

f_s = the sampling rate used,

n = the number of samples used in finding X crossings.

The zero-crossings method can be used primarily for measuring 60 Hz signals on the line. In many cases though, harmonics of 60 Hz may also be present, such as 180 Hz, therefore it would be desirable to measure multiple frequency components. The solution to this was to measure the frequencies in the frequency domain, using the Discrete Fourier Transform (DFT).

4.1.1 DFT

The DFT allows a signal, specified in the time domain, to be viewed in the frequency domain, giving knowledge of the size and frequency of the components of the original waveform. To realize the waveform in the frequency domain, the original signal $x(t)$, must first be sampled to produce the discrete signal $x(k)$. The frequency domain signal $X(n)$ is then calculated by applying the following DFT equation:

$$X(n) = \sum_{k=0}^{N-1} x(k) e^{-j(2\pi/N)nk}, \tag{4.2}$$

where n = the frequency index of the resulting frequency domain signal,

k = the time index of the input data sample,

N = the number of samples used.

Upon completion of the DFT, the sample numbers must be converted to a frequency value over the Nyquist frequency range. For example, if 5000 $X(K)$ samples were taken at a sampling rate of 1024 Hz, then the samples of $X(n)$ would be at intervals of $1024/5000 \approx 0.2$ Hz. Once the peak (or peaks) are located on the $X(n)$ waveform, the sample number n can be translated directly into a frequency the original waveform by multiply n by the interval, 0.2 Hz per sample.

The magnitude of the frequency components can also be determined from the sample spectrum $X(n)$. If it is known that a 1 Vpp, single-frequency sine wave has a

peak magnitude of M_{ref} in the frequency domain, then peaks from the signal $X(n)$ can be referenced to M_{ref} to determine the Vpp of a particular frequency component. For example, if $n = p$ is a point at which a peak occurs in $X(n)$, then $X(p)/M_{ref}$ will be the Vpp of the frequency component represented by $n = p$.

In the case that a peak frequency component fails to fall on a sample in $X(n)$, a method called the Parabolic Fit algorithm (see Section 4.1.2) may be used to estimate the location and magnitude of the peak value.

Verification Results

Simple tests were performed to test the accuracy and reliability of the DFT implementation. The DSP was first used to measure a number of input sinusoidal signals. During the measurement process, the sampled data was transfered to the PC and stored into a file. Once the frequency components of the signal were calculated on the DSP, the results were transfered to the PC for storage. The raw data and the DSP results were used as input, into a MATLAB® program, which could also calculate the frequency components of the raw signal and compare the MATLAB® results with those generated by the DSP.

Comparison tests of the DFT algorithm on the DSP and MATLAB® showed matching results for the same measured input samples, over a frequency range of 100-320 Hz and voltage range from 0.1-7.0 V_{pp}. The results were also compared to the known input waveforms, to verify that both algorithms had correctly calculated the frequency components of the sampled signal.

4.1.2 Parabolic Fit

The Parabolic Fit algorithm is a method of fitting a series of samples to a parabola. The apex of the newly formed parabola represents a closer approximation to the true peak being represented by the samples and hence a better estimate of the true magnitude and frequency of a particular spectral component.

Given a discrete spectrum $X(n)$, the apex of a parabola fit to the peak samples can be found to lie at an offset δ from the peak sample $X(p)$, where $|\delta| \leq 0.5$, by the following formula [20]:

$$\delta = \frac{X(p+1) - X(p-1)}{2[-X(p+1) + 2X(p) - X(p-1)]}. \tag{4.3}$$

The estimate of the frequency index spectral peak is then $D = p + \delta$. The coefficients of the parabola $ax^2 + bx + c$ can then be found by solving multiple equations. Once the equation of the parabola is known, the peak value at the apex can also be determined and used as an approximation for the real signal peak.

Figure 4.1 shows an example in which the parabolic fit, applied to sample numbers 1, 2, and 3, estimates the "true" peak to be at $\delta = -\frac{1}{3}$ from the peak at sample 2. Also, the magnitude of the peak is now approximated by the value 19, at sample $2 + \delta$, rather than the value 18, at sample 2.

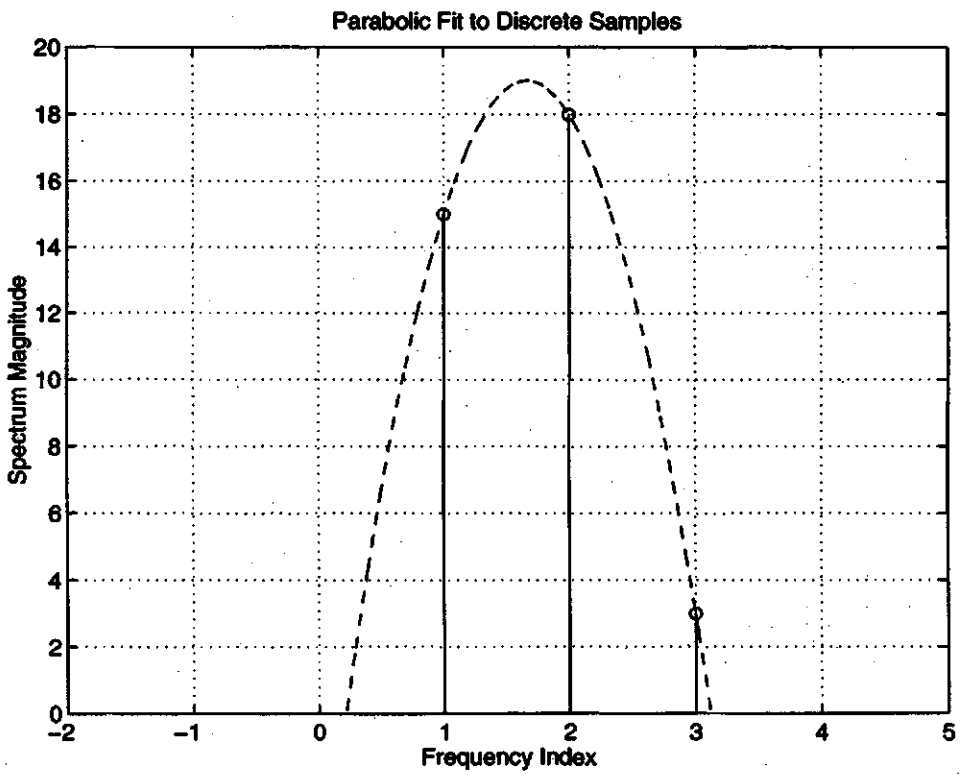

Figure 4.1 Parabolic Fit of Peak to Sampled Data

Verification Results

The parabolic fit algorithm also needed to be verified, so it was tested with MATLAB® and various input data samples. These measurements showed that although the the parabolic fit could determine frequency very accurately, the magnitude that is calculated with this method is not always accurate. Assuming a sampling rate of 1024 Hz, or samples per second, the highest frequency which can be measured at this rate is 512 Hz. This means that 1024 samples are used to represent 512 Hz, or 2 samples per Hz, or an accuracy of 0.5 Hz per sample. As long as the measured frequency is an integer number of Hz or even 0.5 Hz, the frequency and magnitude measurements will be accurate without the parabolic fit. The frequency determination capabilities of the parabolic fit algorithm help when finding a frequency that does not lie on one of the sample points. The magnitude prediction is also useful in this situation, but can result in values being far too low. In the case of the true frequency falling mid-way between two consecutive sample points, the magnitude was measured to be 69% of the actual magnitude. In the more common case where the true frequency does fall on an integer sample point, the magnitude prediction may be useful if the spectral peak has become distorted or spread out by some filtering properties on the line.

4.2 Resistance Measurements

The dc resistance measurement is conducted using a simple voltage divider. A sample rate of 5120 samples per second are used to collect 4096 samples of data. By applying a known voltage V_{in} to a known resistance R_n in series with the unknown resistance R_l, the voltage at the point joining the two resistances can be measured (see Figure 4.2). The unknown value R_l can then be found by using the input voltage V_{in}, the measured voltage V_{meas}, and the known resistance R_n, as shown:

$$R_l = \frac{V_{meas} \cdot R_n}{V_{in} - V_{meas}}. \tag{4.4}$$

In this project, more factors needed to be considered, since the input circuit which

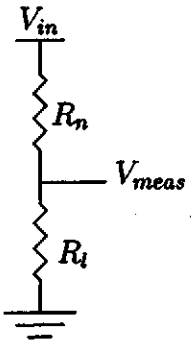

Figure 4.2 A Simple Voltage Divider

is used to scale down the input voltage signals has a resistance which is comparable to those in the voltage divider, as shown in Figure 4.3 (see also Figure A.1). Therefore,

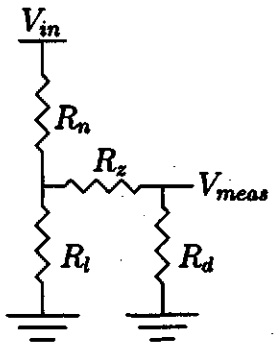

Figure 4.3 The Implemented Voltage Divider

the input resistance $R_z + R_d$ of the measurement circuit must be known and can be used to find R_l as follows:

$$R_l = \frac{V_{meas} \cdot R_n \cdot R_t}{V_{in} \cdot R_d - V_{meas} \cdot (R_t + R_n)}, \tag{4.5}$$

where $R_t = R_z + R_d$.

The problems with this method occur when R_l becomes very large or very small. In one case, R_l is so much larger than the known input resistance $R_z + R_d$ which it is in parallel with, that R_l becomes insignificant in affecting the voltage at the point V_{meas}. This could be solved by increasing R_t appropriately. A new problem is now created though, by the fact that R_t will become comparable to the input impedance

of the voltage-follower, which would affect the signal being passed. The result of this problem become apparent when the results of the measurements are discussed later in Section 5.2.

On the other hand, when R_l is very small, the measured voltage V_{meas} approaches zero. At this point, changes in R_l will cause very little change in the voltage being measured. Therefore, when R_l is measured to be below 7 kΩ[1], a smaller R_n is automatically switched into the divider and the measurement is retaken with more accuracy (again, see Figure A.1).

4.3 Capacitance Measurements

Measurements of capacitance are made by examining the exponential decay of the RC network under consideration. A known voltage V_{in} can be applied to the unknown capacitance, which will then charge up and maintain that voltage until it is allowed to decay through some resistance. Therefore, once the applied voltage is removed the stored voltage decays through the recently measured line resistance R_l and the measurement input resistance R_t. The decaying voltage can then be sampled and used to calculate the capacitance in the calculations which follow.

The decaying voltage is initially sampled at a rate of 5120 samples per second, collecting a total of 128 samples. The first sample is checked to verify that the sampling captured the initial part of the decay. If the first sample is not above a threshold value[2], then the capacitance is recharged and measured again. Upon verification that the first value is valid, the data is again checked to ensure that at least five data samples were taken before the decay passed below one volt. If less than five samples are above the one volt threshold, then the sampling rate is increased to 20480 samples per second and the process is repeated. If needed, a third, final sampling rate of 76800 is used to capture enough samples prior to the voltage decaying to less than one volt. If this highest sampling rate still does not yield five

[1]This value allows the measured voltage to reach ~530mV before switching in the new R_n.

[2]The threshold is based on the supply voltage, minus 50 mV and the drop across the FET's.

samples over one volt, then the capacitance value is considered too small to measure.

Once the data is stored, the analysis can begin. If there is no foreign voltage components in the measured waveform $V_{exp}(t)$, that is no white noise, 60 Hz, etc., then an almost perfect exponential decay will be seen and no further signal processing need occur. The exponential decay has a known mathematical form of

$$V_{exp}(t) = V_{in}e^{\frac{-t}{\tau}} \text{ [3]}, \tag{4.6}$$

where t = time

and $\tau = RC$, the time constant of the system.

From this equation, an unknown value of capacitance C can be found as follows:

$$C = \frac{t}{R \ln \frac{V_{in}}{V_{exp}}}. \tag{4.7}$$

For instance, if $\hat{V}_{exp}(t)$ is measured at a time $\hat{t}$ since the decay began, then C can be found for that sample. By taking a large number of samples at known times, the value of C can be calculated from several of the samples. To help alleviate some of the error caused by noise, calculated values can be averaged to get a better estimate of the capacitance[3].

In a more general case, as described in Section 2.1.3, there will be some noise and possible 60 Hz voltages induced onto the line. To eliminate the effects of the extra signals on capacitance measurements, these extra signals must be removed before the above equations can be used. One method to remove 60 Hz signals, using a 60 Hz filter, is discussed below, in Section 4.3.1.

4.3.1 60 Hz Filter

The obvious choice of signal elimination is a digital filter that is implemented in the DSP. A 60 Hz notch filter would cut out all of the 60 Hz component in the

[3]For a perfect exponential, all calculated values would be the same, therefore multiple values are not necessary.

measured exponential. This eliminates the undesirable components, but the decay itself has some 60 Hz components which would then be missing during the capacitance measurements. Figure 4.4 shows the time domain plot of an expontial decay with 60 Hz noise added, before and after a 60 Hz filter has been applied. Figure 4.5 shows the same waveform in the frequency domain.

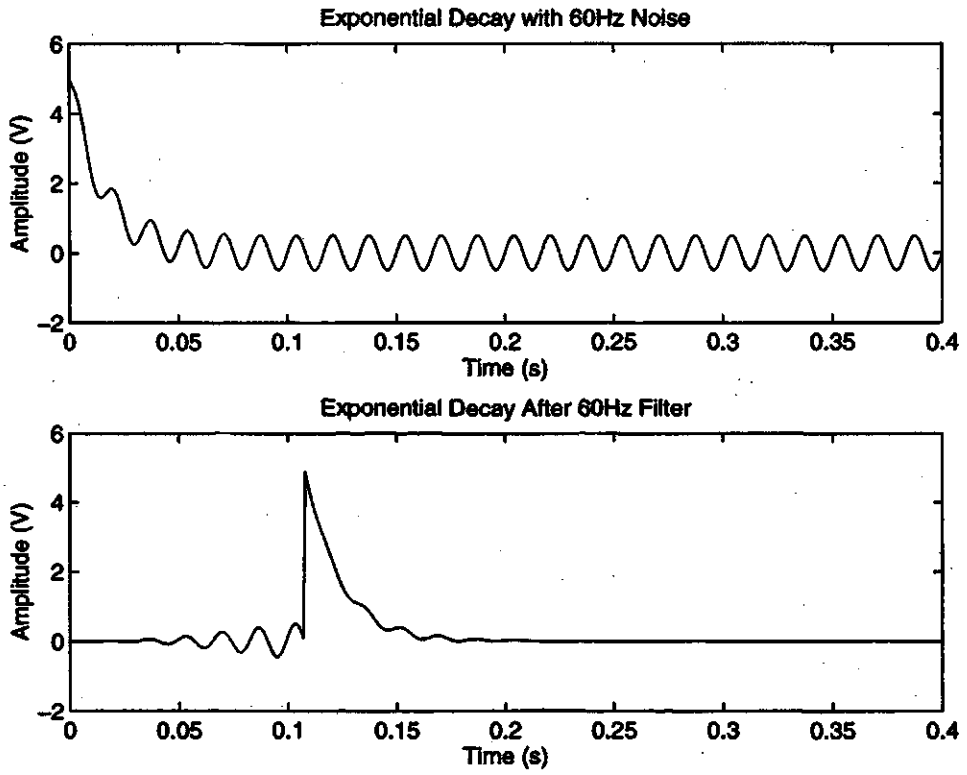

Figure 4.4 Noisy Time Domain Decay Before and After Filter

Although this filter appears to cause as much harm as good, by reversing the filtered signal and passing it through the same 60 Hz filter, the phase distortion is removed and the desired signal, without the 60 Hz noise, remains.

This method is suitable for removing 60 Hz interference, but there is still a problem with harmonics such as 180 Hz and AWGN (additive white gaussian noise), the "random" noise which occurs in any electrical system. Therefore, a better technique than just a single notch filter was necessary to reduce the interference in the measured signal. The solution for this was the Method of Least Squares, as discussed in

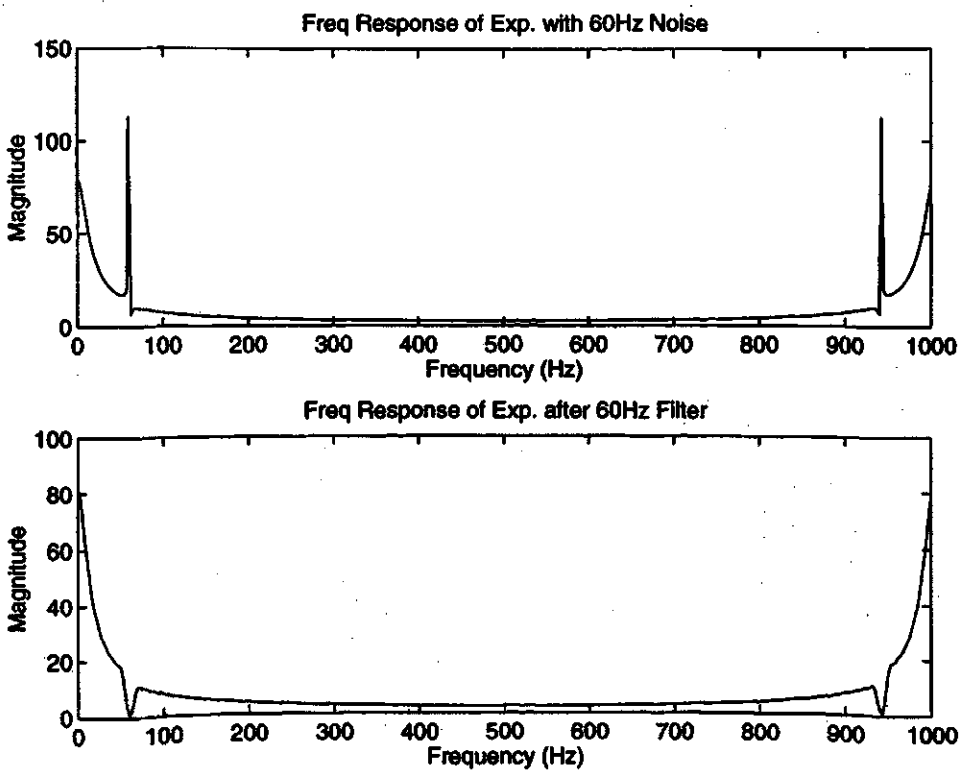

Figure 4.5 Noisy Frequency Domain Decay Before and After Filter

Section 4.3.2 below.

4.3.2 Least Squares

The Least Squares (LS) method can be used to help minimize effects of noise and calculate an accurate capacitance. The simplest form of the LS method is a linear method, therefore the exponential decay must be linearized before the LS alrogithm can be applied. This is done by taking the natural logarithm of Equation 4.6 as shown.

$$\begin{aligned} \ln V_{exp} &= \ln V_{in} - \frac{t}{\tau}, \\ \ln V_{exp} &= -\frac{1}{\tau}t + \ln V_{in}, \end{aligned} \tag{4.8}$$

or

$$Y = b_1 t + b_0, \tag{4.9}$$

where $Y = \ln V_{exp}$,

$b_1 = -\frac{1}{\tau}$,

and $b_0 = \ln V_{in}$.

and $x = t$.

which is the form of an equation of a simple line which must be fit to a perfect straight line.

The idea behind the LS method is to minimize the sum of the squares of the deviation of the measured values y_j from a best fit line. There must be one known variable, which in the case of the exponential decay is the time of the samples t. This leaves the variable containing the error to be the measured values y_j. The error function which the LS method minimizes is then

$$\begin{aligned} \mathcal{E} &= \sum_{j=1}^{N} (y_j - Y_j)^2, \\ &= \sum_{j=1}^{N} (y_j - b_0 - b_1 x_j)^2. \end{aligned} \tag{4.10}$$

where j = the sample number,

x_j = the time at sample j,

and $Y_j = b_1 x_j + b_0$,

= the equation of the line that will minimize the error in sample y_j taken at time x_j

The solution for b_0 and b_1 must be arrived at by solving two equations. One such set of equations can be found by setting the two derivatives of Equation 4.10 to zero, ensuring that the error $\mathcal{E}$ is minimized for both variables. The equations are as follows [21]:

$$\frac{\partial \mathcal{E}}{\partial b_0} = -2\sum_{j=1}^{N}(y_j - b_0 - b_1 x_j), \tag{4.11}$$

$$\frac{\partial \mathcal{E}}{\partial b_1} = -2\sum_{j=1}^{N}[x_j(y_j - b_0 - b_1 x_j)]. \tag{4.12}$$

Setting Equation 4.11 equal to zero, b_0 can be solved for in terms of b_1 as follows:

$$\begin{aligned} 0 &= -2\sum_{j=1}^{N}(y_j - b_0 - b_1 x_j), \\ Nb_0 &= \sum_{j=1}^{N} y_j - b_1 \sum_{j=1}^{N} x_j, \\ b_0 &= \bar{y} - b_1 \bar{x}. \end{aligned} \tag{4.13}$$

where $\bar{y} = \frac{\sum_{j=1}^{N} y_j}{N}$,

and $\bar{x} = \frac{\sum_{j=1}^{N} x_j}{N}$.

The equation for b_1 is still needed and can be found by substituting Equation 4.13 back into Equation 4.10. This then yields

$$\begin{aligned} \mathcal{E} &= \sum_{j=1}^{N}[(y_j - \bar{y}) - b_1(x_j - \bar{x})]^2 \\ &= \sum_{j=1}^{N}[(y_j - \bar{y})^2 - 2b_1(y_j - \bar{y})(x_j - \bar{x}) + b_1^2(x_j - \bar{x})^2]. \end{aligned} \tag{4.14}$$

To ease the process we can perform substitutions on Equation 4.14 as follows:

$$\sum_{j=1}^{N}(a_j - \bar{a})^2 = \sigma_a^2 \tag{4.15}$$

$$\sum_{j=1}^{N}(a_j - \bar{a})(z_j - \bar{z}) = r\sigma_a\sigma_z. \tag{4.16}$$

This allows Equation 4.14 to be rewritten in quadratic form as shown [22].

$$\mathcal{E} = \sigma_y^2 - 2b_1 r\sigma_x\sigma_y + b_1^2\sigma_x^2 \tag{4.17}$$

By taking the derivative of Equation 4.17 with respect to b_1, setting it equal to zero, and solving for b_1, the following results:

$$b_1 = \frac{r\sigma_y}{\sigma_x}. \tag{4.18}$$

Substituting back in from earlier simplifications, we are left with

$$b_1 = \frac{\sum_{j=1}^{N}[(x_j - \bar{x}) \cdot (y_j - \bar{y})]}{\sum_{j=1}^{N}(x_j - \bar{x})^2}. \tag{4.19}$$

Equation 4.13 and Equation 4.19 now define the line for known values of x. The value of τ can now be solved using Equation 4.8. C can then be easily be found since the R of the system is already known from previous measurements.

Verification Results

In the actual tests, a modified LS algorithm was used. The modified LS algorithm uses a fixed y-intercept, which is achieved by using a known value of b_0 in Equation 4.9. This can be done because the initial value of the exponential decay is a known value[4].

To test this algorithm, the DSP test set was first used to measure the capacitance in an RC configuration. The sampled data, along with the results, were then fed into MATLAB® where noise was added and the algorithm applied. Figure 4.6 shows a specific instance of the input RC exponential decay, with and without some added noise[5]. Also shown is the resultant decay after applying the LS method to the noisy input (indicated by Final Output).

[4]The known value is 8 V, since this is the supply voltage which is being used to charge the line

[5]The added noise includes a 2 V_{pp} 60 Hz sinusoid plus AWGN with a 0.5 V standard deviation.

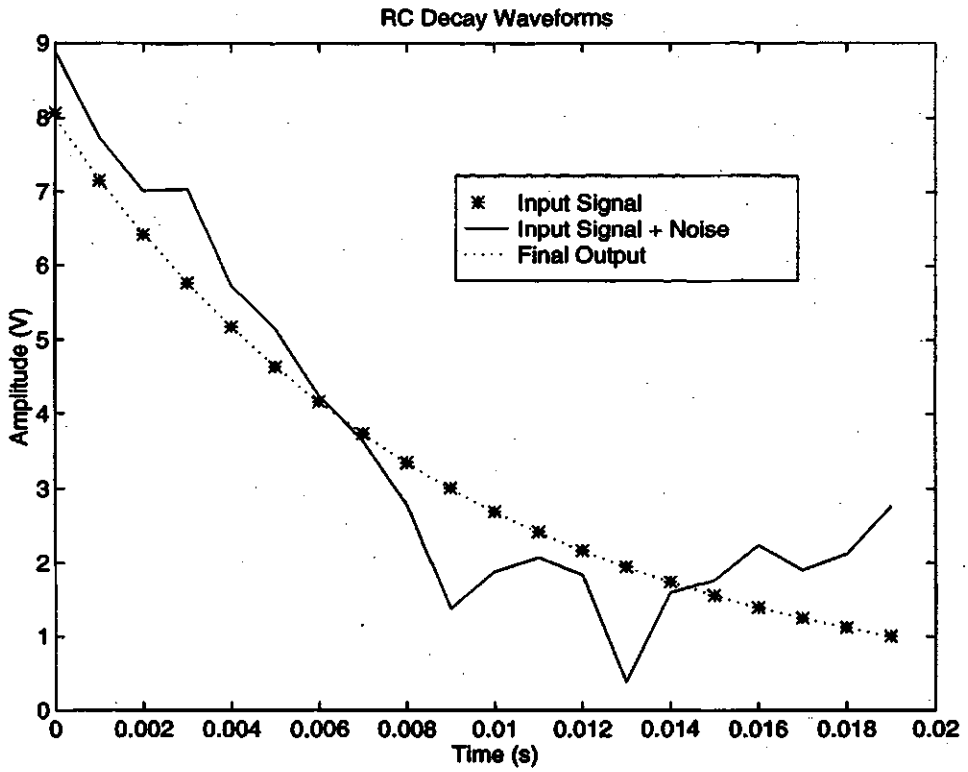

Figure 4.6 Exponential Decay with AWGN and 60 Hz

The modified LS method is then applied to the noisy waveform, to try to determine the capacitance value which would most likely create such a decay. The data is first linearized (see Section 4.3), which is shown in Figure 4.7. This data shows the linearized waveforms of the original decay, the noisy decay, and the resultant decay after the modified LS algorithm has been applied. As can be seen, the noisy data in Figure 4.6 results in an equally noisy line in Figure 4.7. The modified LS method smooths out this line, based on the calculation of the least squares error. An unmodified version of the LS method, would also result in a straight line, but since the original level before decay is known, the y-intercept b_0 of the line can be set instead of calculated.

The calculated capacitance values are plotted in Figure 4.8. The solid line represents the capacitance value found by applying Equation 4.7 to each measurement sample. The dashed line shows the estimated capacitance value using the modified LS method, Equation 4.13, and Equation 4.9. The plot obviously indicates that the

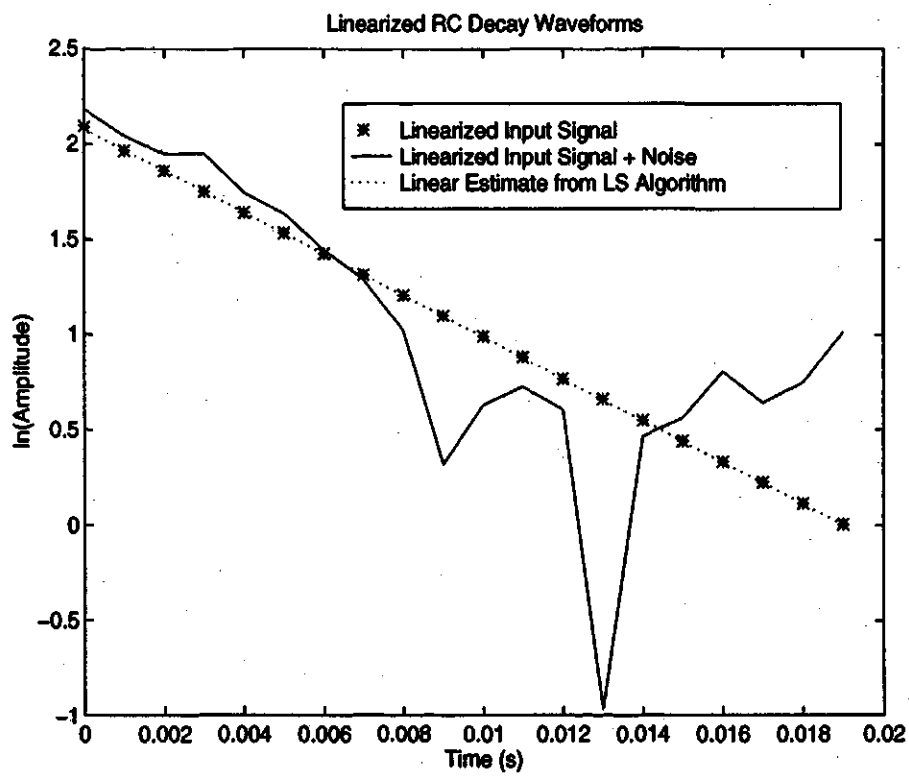

Figure 4.7 Linearized Exponential Decay with AWGN and 60 Hz

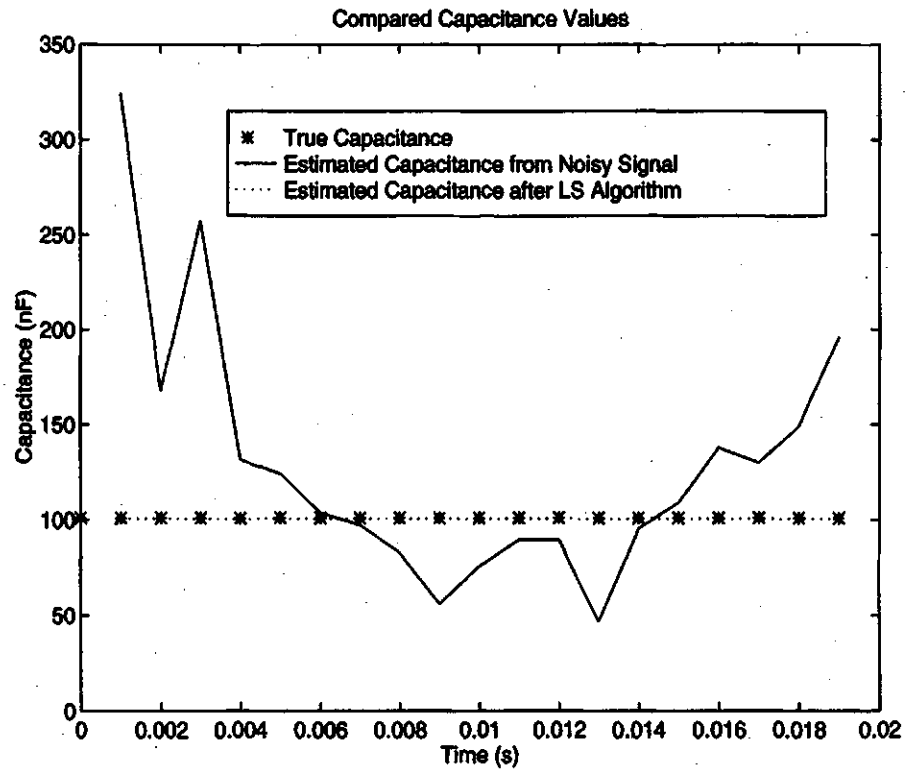

Figure 4.8 Estimated Capacitance Using Modified LS Method

LS method is capable of removing the undesired noise and results in an approximate measure of the true capacitance found in the original RC decay. The small difference between the actual capacitance and the measured value, as seen in Figure 4.8, may be attributed to the limited number of samples which are used to minimize the error in the linearized data.

4.4 Calculating Line Model Parameters

The line model parameters which are being measured in this project include the components in the equivalent circuit shown in Figure 4.9. The testing process which

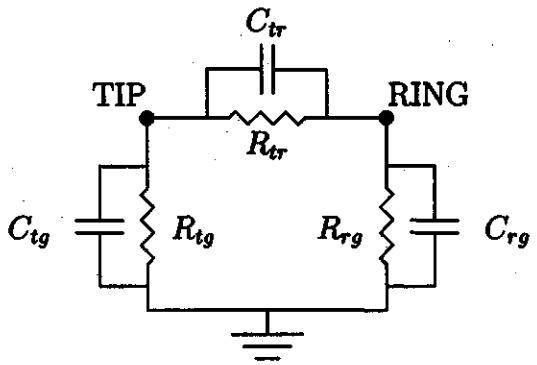

Figure 4.9 Equivalent Circuit

takes place measures combined parameters of the circuit. Looking at the resistance measurements, there are three parameters which must be measured. Solving for three unknowns requires three equations, which can be found by making three measurements of different configurations of the circuit. Solving these equations leads to the desired resistance values. Following this, three measurements are again made of combined capacitances. With three equations, the desired capacitance values can also be solved.

The three configurations used in making measurements include connecting tip to ground and making measurements between ring and ground, connecting ring to ground and making measurements between rip and ground, and connecting tip to ring and making measurements between tip and ring to ground. Making measurements

with tip grounded, we will see $R_{tr}\|R_{rg}$ and $C_{tr}\|C_{rg}$. The other configurations will give $R_{tr}\|R_{tg}$, $C_{tr}\|C_{tg}$, $R_{tg}\|R_{rg}$, and $C_{tg}\|C_{rg}$. The equations for parallel resistance and capacitance, along with the measured values, produce the sets of three equations. The final equations used are then

$$R_{tg} = \frac{2}{C^{-1} - B^{-1} + A^{-1}}, \tag{4.20}$$

$$R_{rg} = \frac{1}{B^{-1} - A^{-1} + G_{tg}}, \tag{4.21}$$

$$R_{tr} = \frac{1}{A^{-1} - G_{tg}}, \tag{4.22}$$

where A = measured resistance with ring grounded ($R_{tr}\|R_{tg}$),

B = measured resistance with tip grounded ($R_{tr}\|R_{rg}$),

C = measured resistance with tip shorted to ring ($R_{tg}\|R_{rg}$),

and $G_{tg} = R_{tg}^{-1}$, the conductance from tip to ground,

and

$$C_{tg} = \frac{Z - Y + X}{2}, \tag{4.23}$$

$$C_{rg} = \frac{Y - X + Z}{2}, \tag{4.24}$$

$$C_{tr} = \frac{X - Z + Y}{2}, \tag{4.25}$$

where X = measured capacitance with ring grounded ($C_{tr}\|C_{tg}$),

Y = measured capacitance with tip grounded ($C_{tr}\|C_{rg}$),

and Z = measured capacitance with tip shorted to ring ($C_{tg}\|C_{rg}$).

These equations were solved using MATLAB®, since the current implementation of the DSP code is only capable of gathering one set of resistance and capacitance.

4.5 Summary

Algorithms were implemented both on and off the DSP chip to estimate the required parameters. The algorithms range from relatively simple to more theoretically

complex. The software implemented these algorithms to help determine various measurement parameters, including voltages and line capacitances and resistances. Final calculation of resistance and capacitance was done external to the DSP module due to constraints in the prototype DSP code.

5. MEASUREMENT RESULTS AND DISCUSSION

Measurements were conducted in the laboratory to test the accuracy and robustness of this design. Known components and voltages were used to prove the accuracy of the measurement, while twisted pair wire was used to simulate a subscriber loop for practical measurements. Faults were also generated on the loop so the data could be analyzed for fault diagnosis. This chapter will look in detail at the results from these tests.

Sections 5.1 and 5.2 describe the use of the DSP tester to measure known dc/ac voltages, resistances, and capacitances. The setup for these measurements is shown in Figure 5.1.

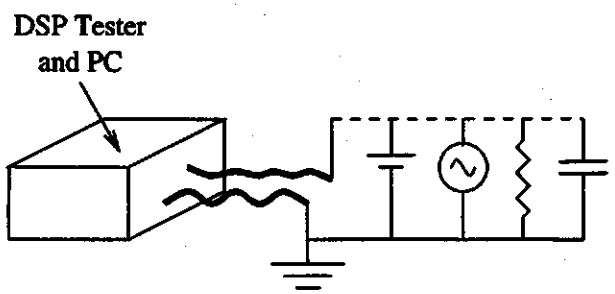

Figure 5.1 Test Setup for Tester Verification

5.1 Voltage Measurements

Testing the loop tester with known voltages was the key to ensuring accurate measurements later. Knowing that the measured input values were correct, the algorithms could be debugged appropriately.

Voltage measurements which were tested included dc levels, ac levels, and ac

frequency [1]. Tests were conducted by applying a known voltage to the input test leads. For dc measurements, input voltages between -8.0 and +8.0 V were used. Each dc voltage was measured 5 times to show the consistency of the results. Peak-peak voltage levels were varied between 0.0 and +8.0 V for the ac measurements. The ac signals were also measured 5 times at each level, with the ac frequency being changed for each of the 5 measurements. Frequencies used for the ac voltages were 60 Hz, 103 Hz, 151 Hz, 199 Hz, and 247 Hz.

Figure 5.2 shows plots of both the dc and ac measurements. Each set of measure-

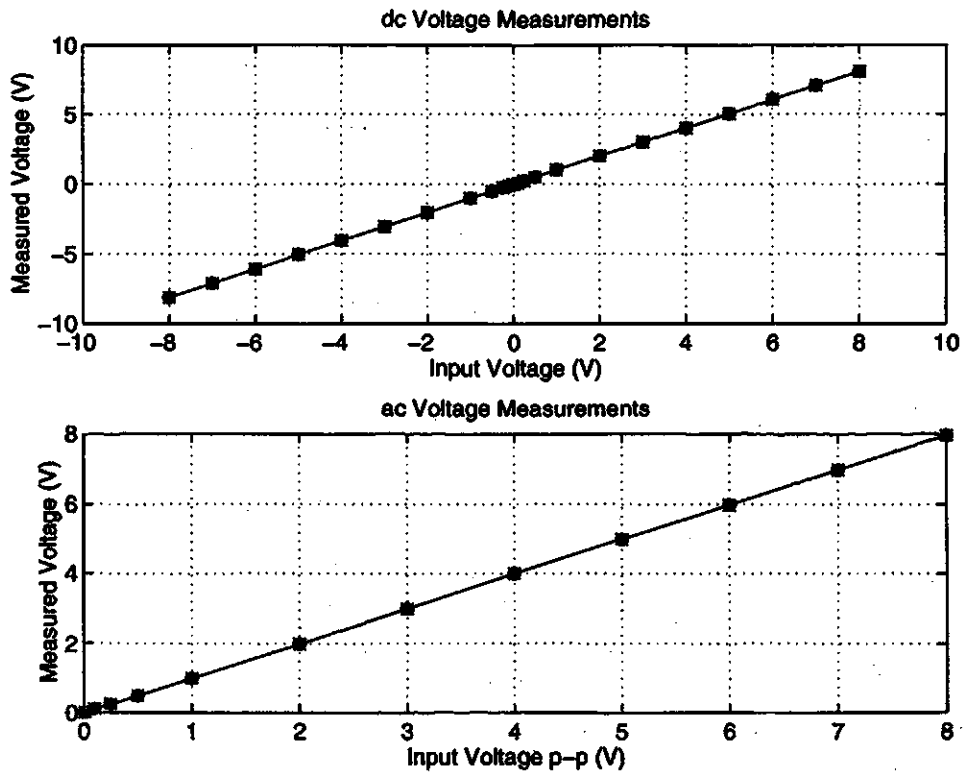

Figure 5.2 dc and ac Voltages Measurements

ments has been plotted and the data points have been connected with a line, to show the linearity of the results. All 5 sets of results appear on the same graph (including the 5 different frequencies used for the ac signals), but cannot be distinguished due to the precision of results and scale of the graph.

There is actually some deviation between the input and measured value, as can

[1]The original tabulated results are included in Appendix B.

be seen in the error plots in Figure 5.3 and Figure 5.4. The error is shown for all 5 sets of measurements taken [2], which includes the error for various frequencies during the ac measurements. The dc values actually vary linearly from the input voltages

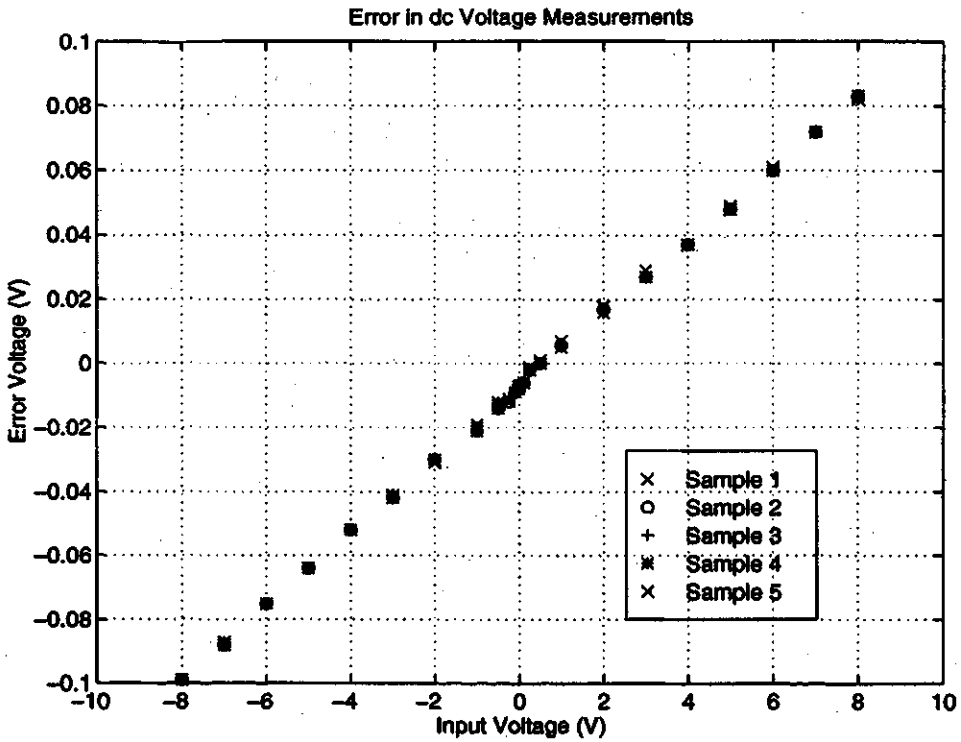

Figure 5.3 dc Voltage Measurement Error

and there is also a slight dc offset when the input is grounded. For negative inputs voltges, the dc value is in error approximately 1.25%, but is closer to 1% for positive values. The ac voltages, measured using the DFT algorithm, also show a growing deviation as the magnitude of the input increased. The ac error only affects the ac voltage measurements, since this is the only time the DFT is used in a measurement. On the other hand, the dc error affects the resistance and capacitance measurements as well, since both of these measurements are conducted in an identical manner as the dc tests. Consequently, the resistance and capacitance measurements can be expected to have some error, due to the known error in making dc voltage measurements.

[2]Only 4 ac error values were plotted, due to the inability to distinguish the 5th set of data.

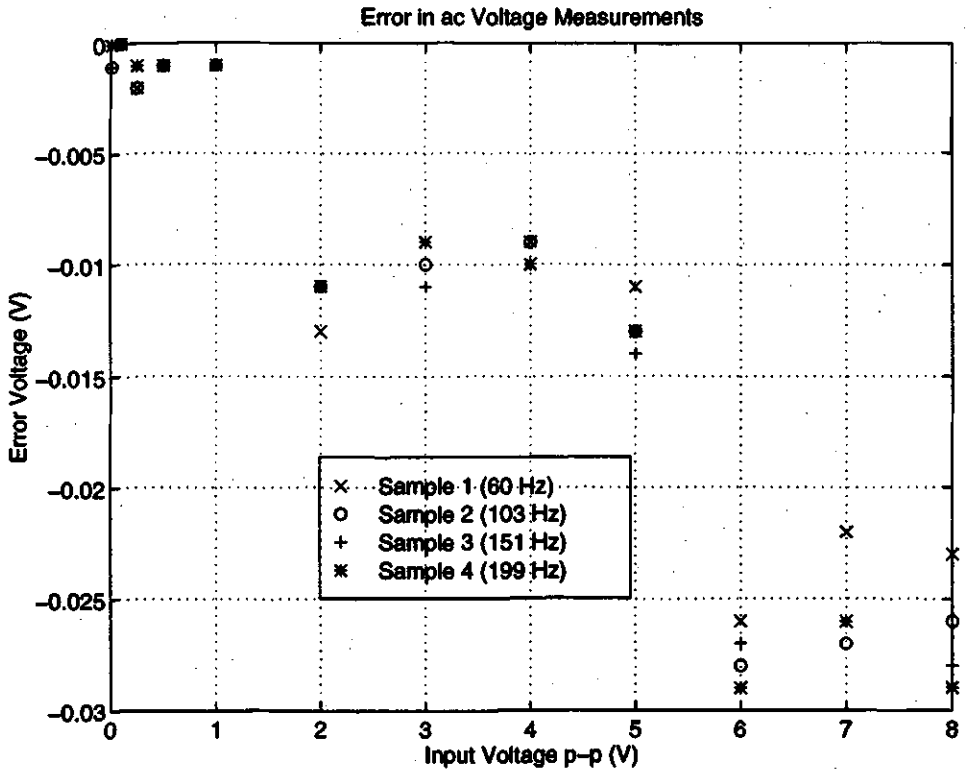

Figure 5.4 ac Voltage Measurement Error

5.2 Component Measurements

Component measurements were done by connecting known resistors and capacitors to the test leads. The components used covered the range of values expected to be found on the subscriber loop. Eight different values of resistors were used and four different values of capacitors. As described in Section 4.2, the resistances were measured with a simple voltage divider, therefore the result relied directly on the accuracy of measuring the dc voltage between the resistors involved. Recall also (from Section 4.2), that large resistances may not measured accurately. Figure 5.5 and Figure 5.6 show the sampled values in Ohms (indicated by *) along with the actual value of the component (dashed). Twelve measurements were taken for each of the eight resistors. It should be noted that the resolution is only 1 kΩ for any resistance greater than 32767 Ω, which is the greatest number that can be sent from the DSP to the PC via the signed 16 bit format. Therefore, a scaling factor of 1000 was used to scale down any values greater than the 32767 limit. The percentage error

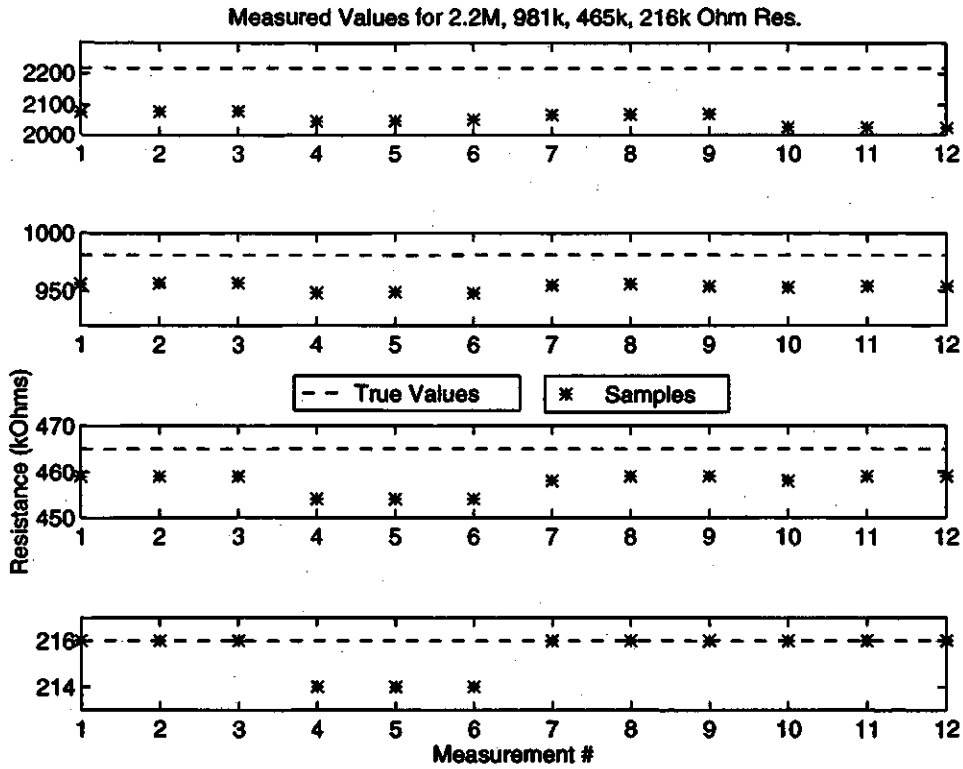

Figure 5.5 Resistor Measurements

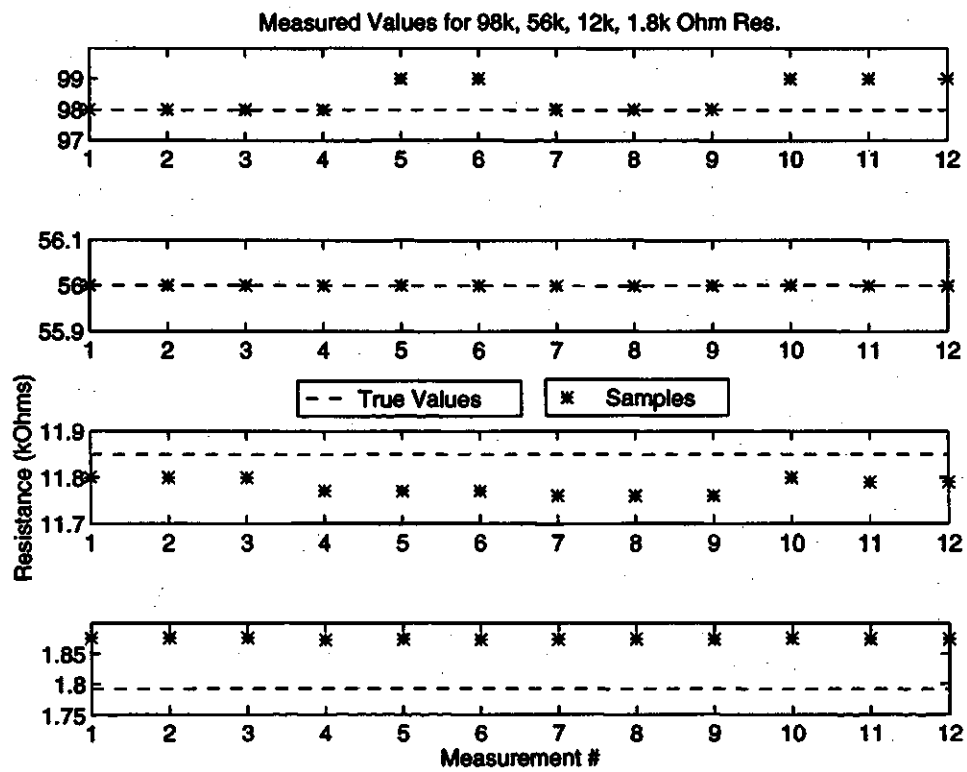

Figure 5.6 Resistor Measurements

of the worst case measurement for each resistance is shown in Table 5.1 below, along with the error of the average measured value.

Table 5.1 Resistance Error Percentage

	Resistance Being Measured (kΩ)							
	2200	**981**	**465**	**216**	**98**	**56**	**12**	**1.8**
Worst Case % Error	8.78	3.36	2.28	1.11	.75	.72	.76	4.69
% Error of Average	7.35	2.81	1.51	.42	.16	.72	.58	4.60

The capacitor measurements were conducted as described in Section 4.3, using the Least Squares method to fit the best exponential to the measured decay. Data was compiled for four different capacitors using 24 measurements each, with results shown in Figure 5.7. The results of the capacitance measurement also relies on the

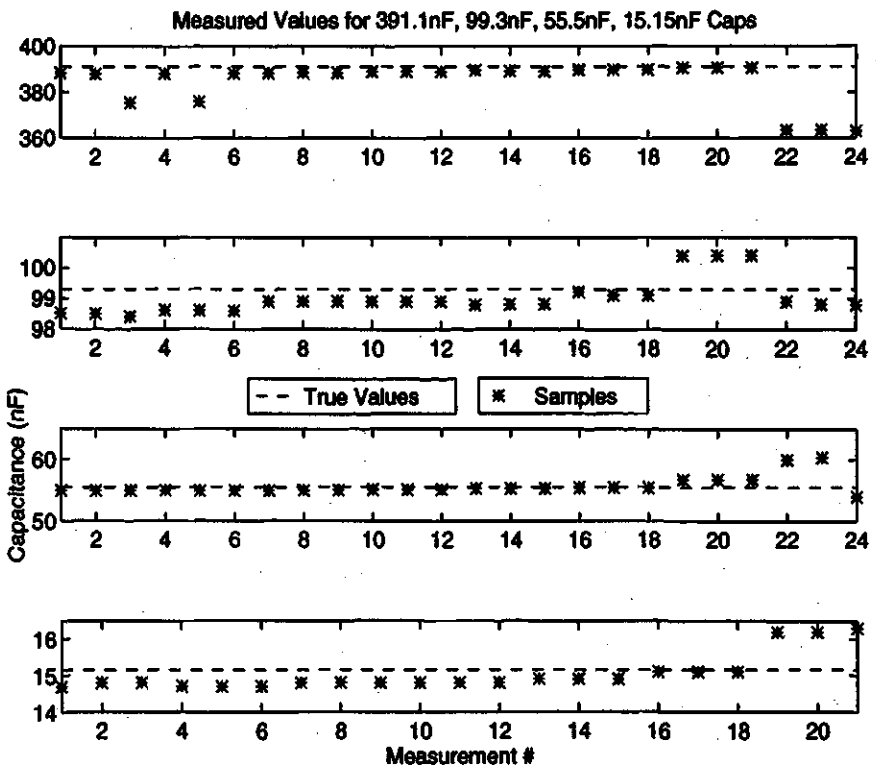

Figure 5.7 Capacitor Measurements

resistance value being used and how accurately it was measured. The decay which is being sampled is a result of the combined RC circuit and the calculations which are

used are based on the result of the resistance measurement. However, when measuring large resistances in combination with the capacitance, the resistance again has little effect since it is the parallel resistance with the voltage-follower input which causes the main part of the decay. Table 5.2 shows the percentage error for the worst case capacitance measured for each capacitance value, along with the percentage error of the average measured value.

Table 5.2 Capacitance Error Percentage

	Capacitance Being Measured (nF)			
	391.1	**99.3**	**55.5**	**15.15**
Worst Case % Error	7.16	1.11	8.83	7.59
% Error of Average	1.62	.30	.39	.71

Overall, the accuracy of the component measurements allows useful data collection on the subscriber loop. The next section examines data taken from an actual twisted-pair cable, in laboratory conditions.

5.3 Loop Measurements

Following verification of the DSP-based tester using known components, tests where conducted in the laboratory on a bundle of twisted-pair cable. A large array of tests were conducted using DSP-based tester, some of which were then verified using a precision laboratory measurement device [3]. Noise, including 60 Hz and AWGN, was not added to the subscriber loop for these measurements, in order that the basic measurements of the DSP-based tester on the subscriber loop could be verified with minimal interference.

The test setup was similar to that shown in Figure 5.1, but instead of testing known voltages and components, the test leads were connected to the twisted-pair. The following sections discuss the process and results of these tests.

[3]The original tabulated data measurements are included in Appendix C.

5.3.1 DSP Measurement Results

The subscriber loop measurements were performed in the laboratory at TRLabs Saskatoon, on Canada Wire 26 gauge, 11 conductor twisted pair cable. Characteristics of the 26 gauge line include specifications of 52 nF/km and 270 Ω/km [7]. Line lengths of 715 m and 1120 m were used in combination to produce a range of line lengths up to 5005 m. Parameters were measured for the various lengths of line, first without fault and later with two fault conditions. Faults were generated from tip-ring and from tip-ground. In both instances, the fault varied in resistance from 100 kΩ to 1.8 kΩ and was introduced at all possible lengths along the loop. For example, if a line length was made up of three 1120 m lengths, then the fault would be placed at 3360 m, 2240 m, and 1120 m, by simply connecting the known fault resistance to the same contacts that were used attach the individual sections of line. The subscriber end of the loop was connected to a Nortel Networks Corp. Unity model telephone with electronic ringer.

Measurements of the line were made in three separate stages, due to the fact that only one RC is measured each time the program is run, as described in Section 4.4. Measurements were taken between tip-ring, tip-ground, and ring-ground, before being evaluated in MATLAB® for the final parameters to be calculated, as described in Section 4.4.

Results from the first set of measurements can be seen in Figures 5.8, 5.9, 5.10, and 5.11. These figures show measured tip-ring capacitance values [4] when a short circuit is made with varying resistor values of 1.8, 12, and 98 kOhms, between the tip and ring wires, or the tip wire and ground. For example, in Figure 5.8, the top plot shows the tip-ring capacitance measurements for a line which is 2145 metres in total length. The solid line connects 3 measurements made when shorting the tip and ring wires with the varying resistances, at a distance of 2145 metres. The dashed line shows the same 3 measurements, when the short circuit occurs at 1430 metres, while

[4]Only 3 measurements make up each line in these plots, but they have been connected in a piece-wise manner to show the general trend of the data.

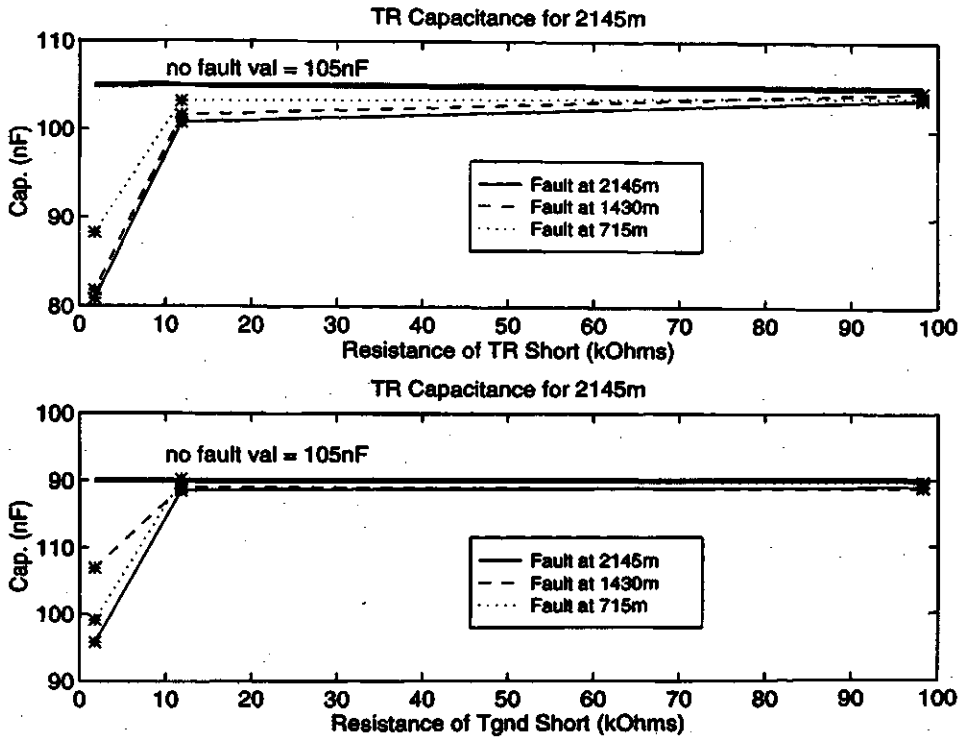

Figure 5.8 TR Capacitance for 2145 m

the dotted line is made by short circuiting at 715 metres. The bottom plot in the same figure was made by similar measurements, but the short was made between the tip wire and ground. The other 3 figures show similar measurements, but are based on varying total line lengths. In all 4 graphs, a general trend can be seen - for smaller fault resistances the TR capacitance seems to follow a decreasing, exponential type curve. Another observation is that the capacitance estimate increases slightly as the distance to the fault nears the measurement end.

The only resistance measurements which turned out to be of any interest are shown in Figures 5.12 and 5.13 [5]. All of these plots show how the specified measured resistance varied with the fault resistance [6]. The only difference between the measured and actual fault resistance is the additional resistance added by the length of line used in the measurement. For TR faults, additional resistance of the loop from the

[5]The other measurements using larger fault resistances all came out to be high impedance, which matches results from a non-faulted loop.

[6]Resistances of 1.8, 6.8, 12, 22, and 98 kOhms were used to create the fault.

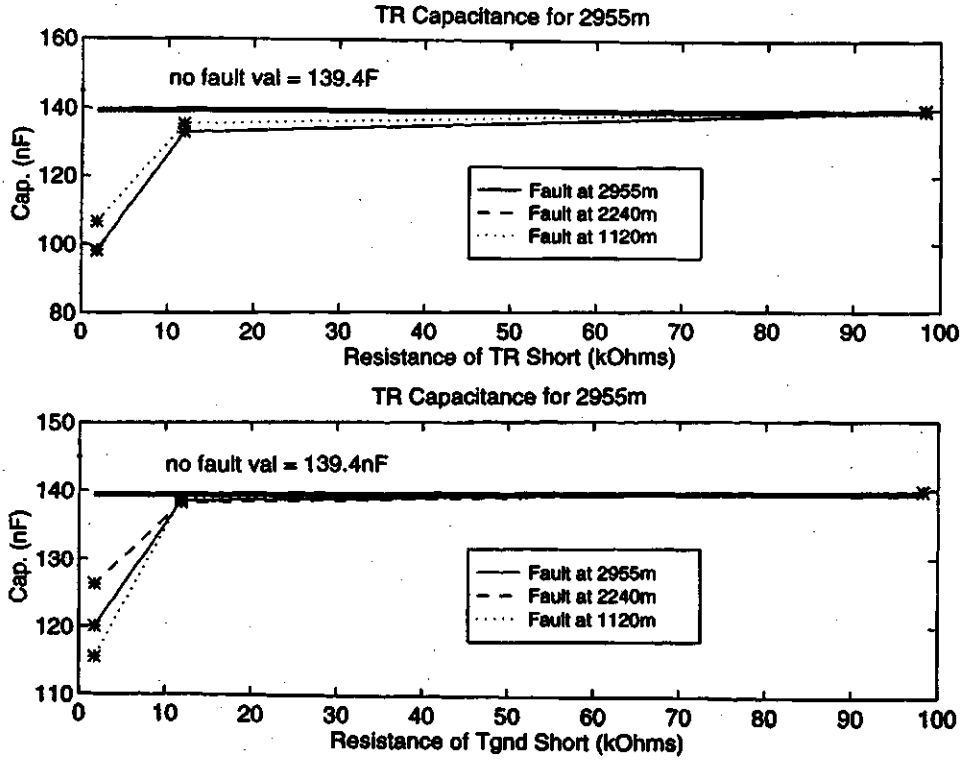

Figure 5.9 TR Capacitance for 2955 m

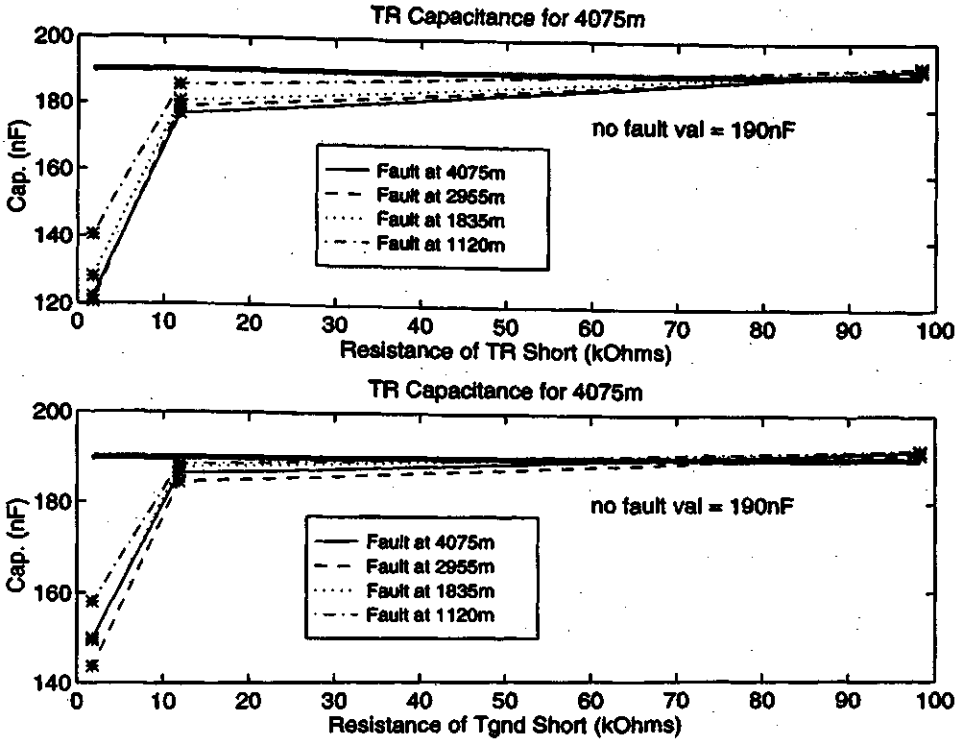

Figure 5.10 TR Capacitance for 4075 m

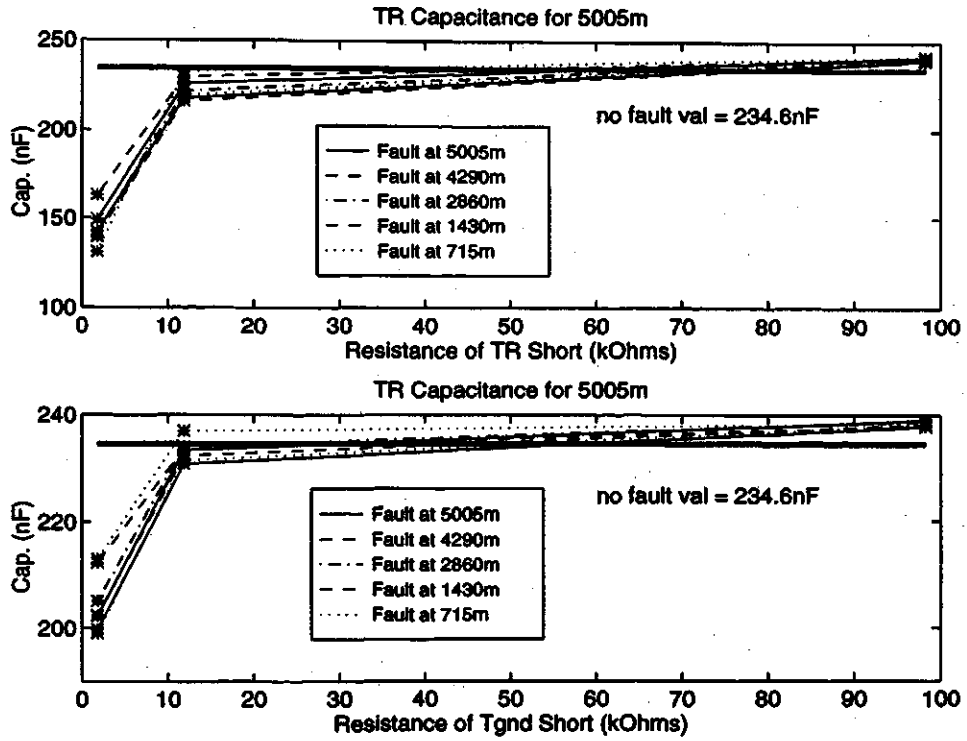

Figure 5.11 TR Capacitance for 5005 m

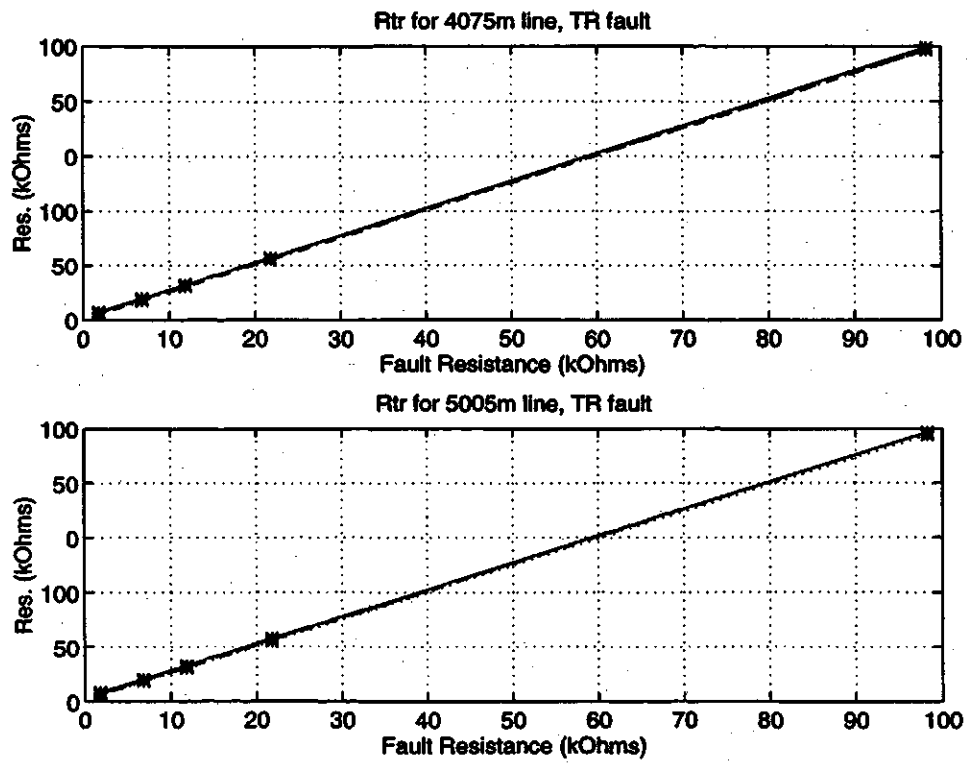

Figure 5.12 TR Resistance for TR Fault

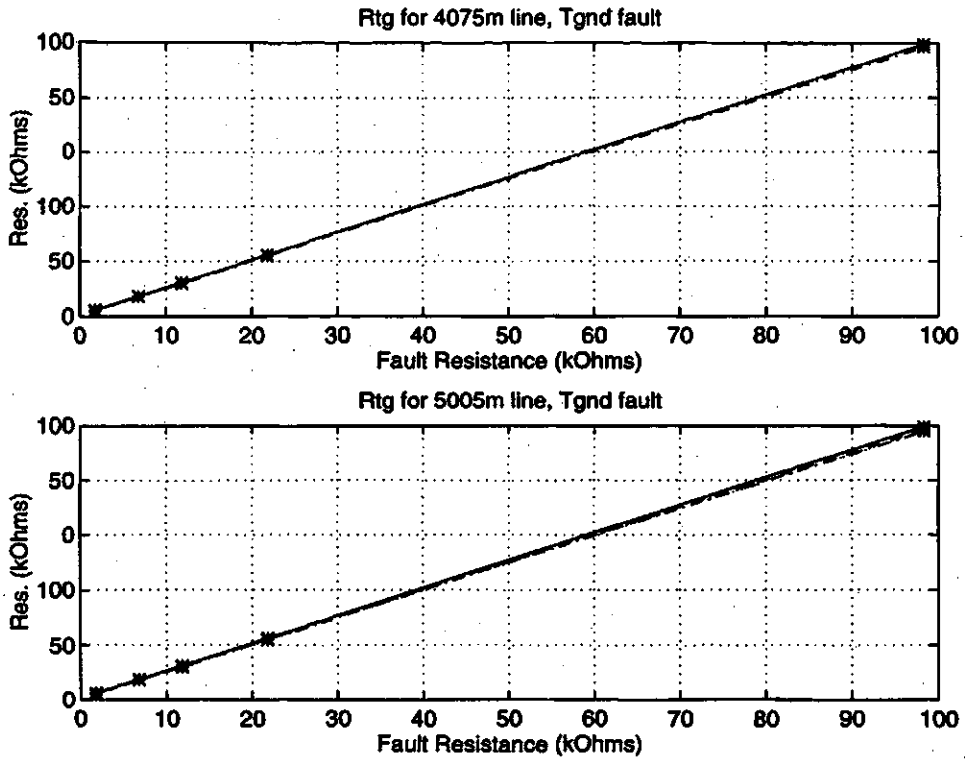

Figure 5.13 Tgnd Resistance for Tgnd Fault

measurement end to the fault and back, is measured. Tip-ground faults only measure the one-way resistance of the loop. Plots of the 5005 meter loop include data taken for fault occurences at 5005, 3575, 2145, and 715 meter lengths. 4075 meter plots have fault occurences at 4075, 2955, and 1120 meters.

When a loop is analyzed, with either a tip-ring or tip-ground fault, the resistance measurements can therefore be used to determine the type and resistance of the fault. The resistance of the fault will not be exact, for reasons described above, but will help in determining fault location using the capacitance plots.

To gain a better understanding of the plots shown in Figures 5.8, 5.9, 5.10, and 5.11, a second set of data was taken which consisted of five measurements for each individual fault condition. This time, measurements were taken for only two lengths of line: 5005 m and 4075 m. Also, five different fault resistances [7] were used to help smooth out the capacitance plots. The resulting plots were easier to read and made

[7]Resistances of 1.777, 6.813, 11.84, 21.8, and 98.3 kOhms were used.

the observations more obvious.

Figures 5.14, 5.15, 5.16, and 5.17 show the tip-ring capacitance measurements for tip-ring and tip-ground faults. Results are similar to those shown in Figures 5.8,

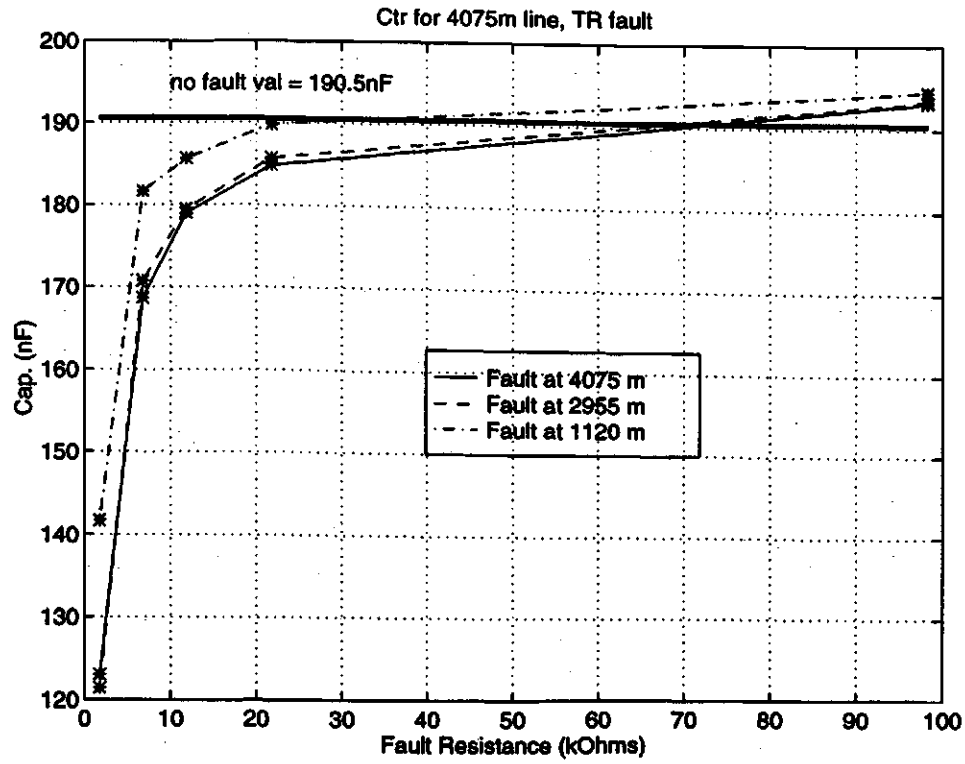

Figure 5.14 TR Capacitance for TR Fault

5.9, 5.10, and 5.11, although these newer results are the output of a five measurement average. The thick horizontal line shown on these plots is the value that was measured for a "clean" line with no faults. As before, the capacitance can be seen to decrease as the fault resistance decreases, with an almost exponential decrease below approximately 30 kΩ [8]. Also, as the location of the fault moves closer toward the measurement end the capacitance seems to increase slightly for the same resistance.

The change in estimated capacitance as a result of the change in fault resistance is a very non-intuitive outcome[9]. Similar results can also be seen in the tip-ground

[8]Note that direct shorts were not tested since they would result in railed values.

[9]Capacitance of a completely shorted line was not measured, due to the speed at which the decay would have to be sampled to get an accurate measurement.

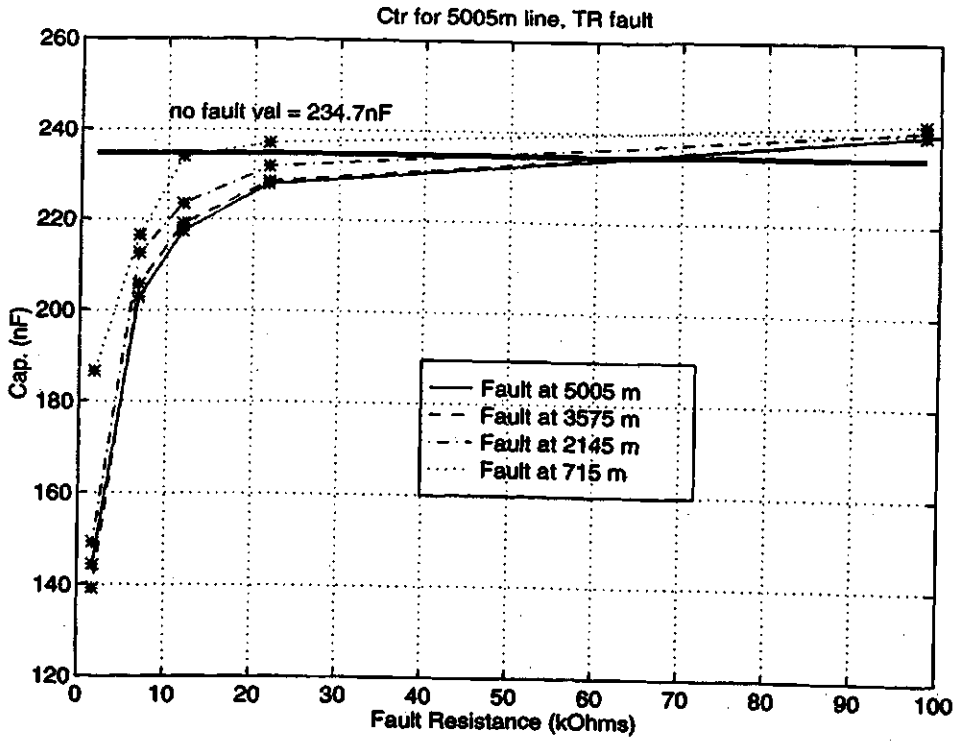

Figure 5.15 TR Capacitance for TR Fault

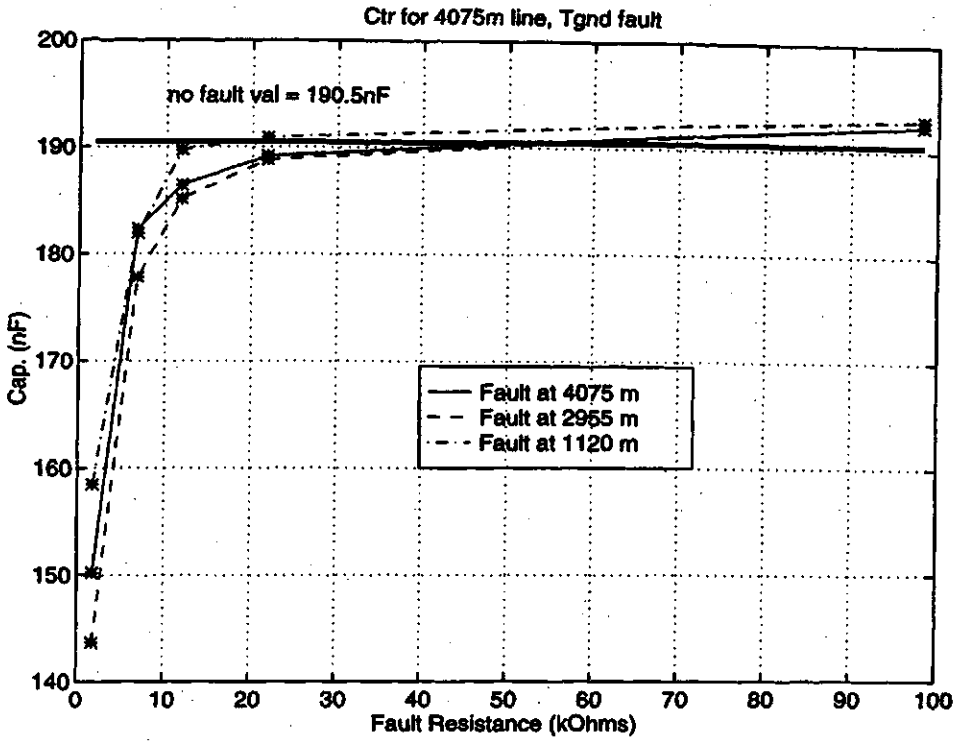

Figure 5.16 TR Capacitance for Tgnd Fault

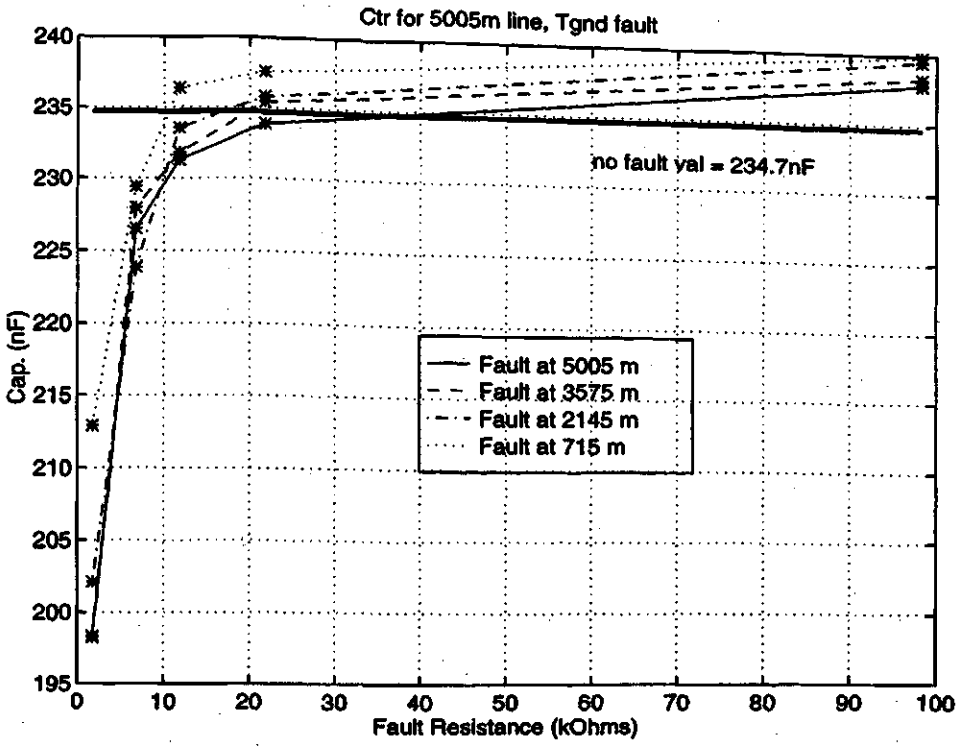

Figure 5.17 TR Capacitance for Tgnd Fault

and ring-ground capacitances for a tip-ground fault. These results are shown in Figures 5.18, 5.19, 5.20, and 5.21. The curves are similar to the tip-ring capacitance plots with the added oddity of showing negative capacitance. It should be noted that the negative capacitance was not a directly measured value, but was a result of the calculations based on the model shown in Figure 2.3.

The effect of the changing resistance on the capacitance and the negative capacitances may be a result of the same, "unknown cause". One theory which may have led to such results, was that the subscriber telephone on the end of the line had active components which may have had an impedance (including capacitance) change caused by a varying current flow, utlimately caused by a changing resistance. This was proven not to be the case when tests were redone with and without the telephone connected and no differences were observed.

The most likely cause for such results may be an incorrect line model. Accuracy of the tests were proven during earlier measurements and raw data found by the

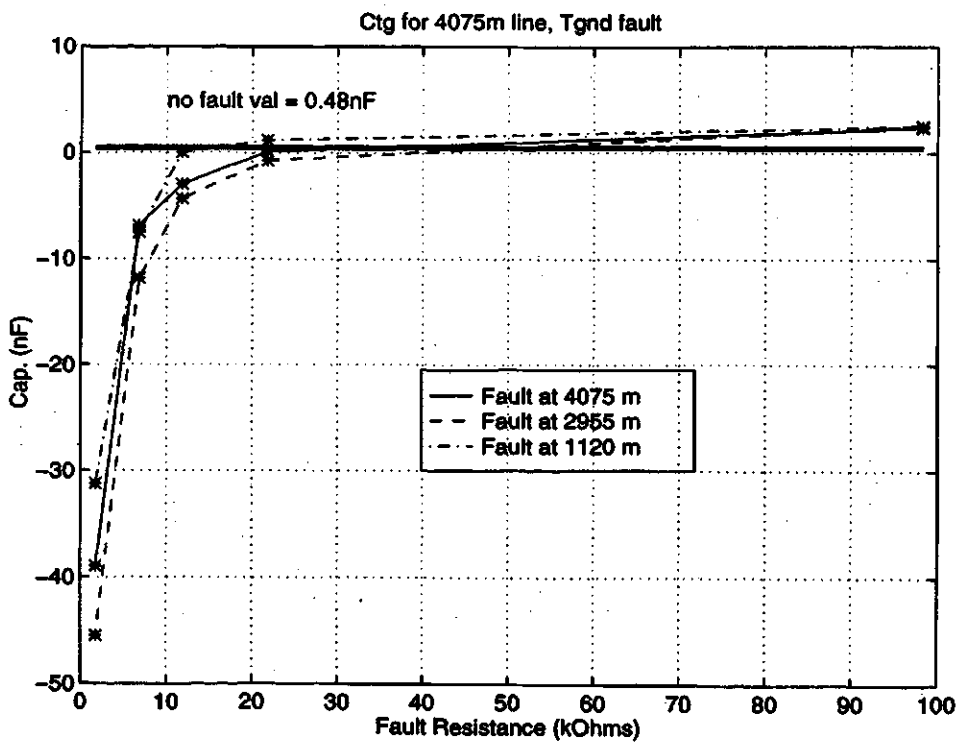

Figure 5.18 Tgnd Capacitance for Tgnd Fault

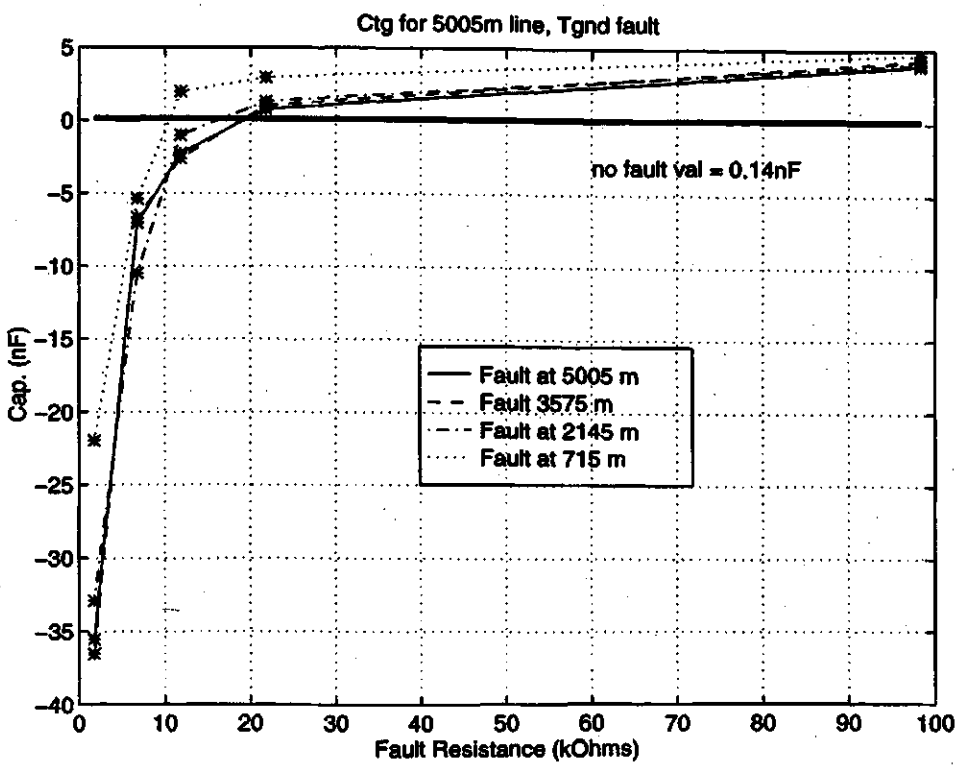

Figure 5.19 Tgnd Capacitance for Tgnd Fault

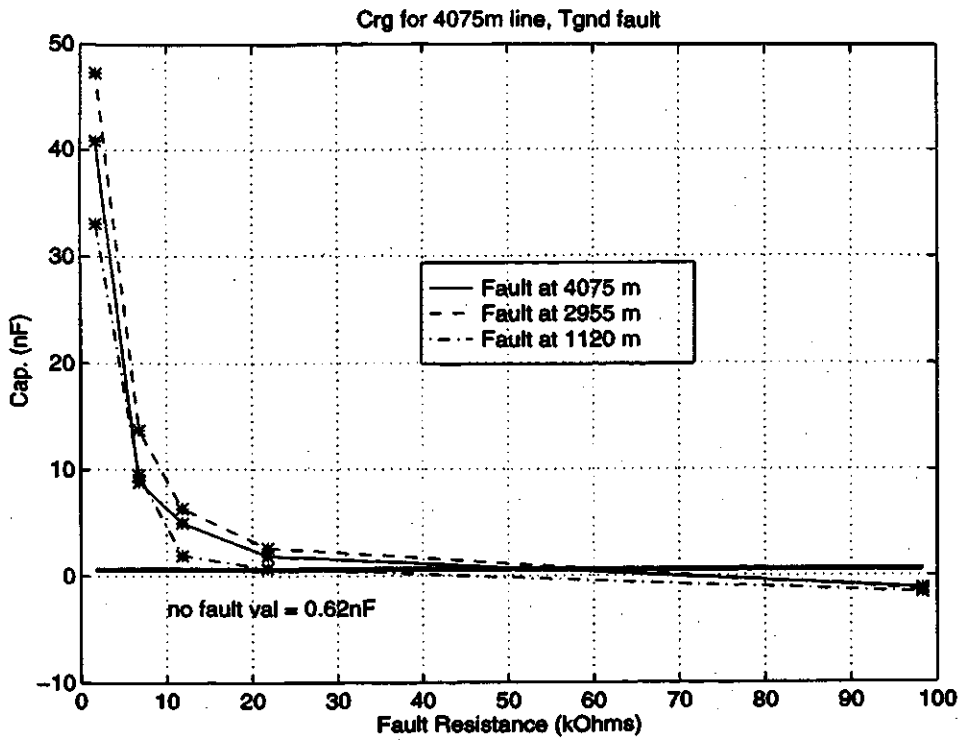

Figure 5.20 Rgnd Capacitance for Tgnd Fault

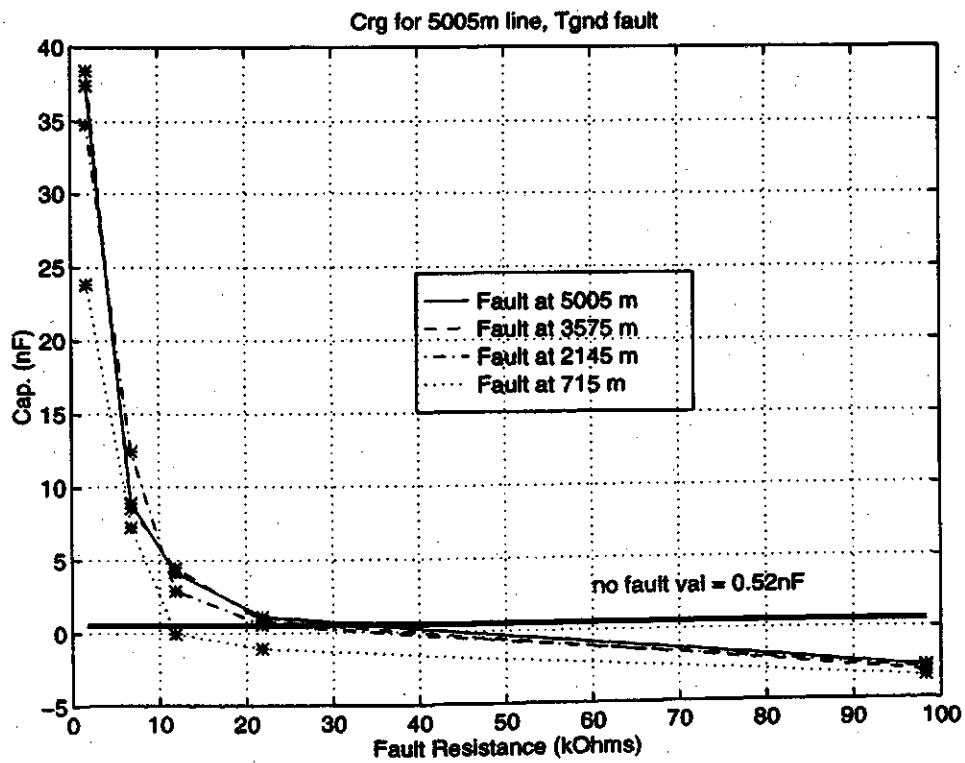

Figure 5.21 Rgnd Capacitance for Tgnd Fault

test seemed reasonable. The odd final results stemmed from a series of calculations based on the equivalent circuit model, which was assumed since the beginning of the project [10]. In other words, since the calculations which produce the results, such as negative capacitance, are derived based on the equivalent circuit, it is highly likely that the equivalent circuit is not accurate.

A more accurate line model may be one which assumes a distributed capacitance, although this makes calculations much more difficult [6]. In a distributed model, each small section of a transmission line can be shown as in Figure 5.22, where Δx is the length of the section, $g\Delta x$ is the conductance from the line to ground, $c\Delta x$ is the capacitance from the line to ground, $l\Delta x$ is the inductance along the section of line, and $r\Delta x$ is the resistance along the section of line. By connecting many sections of

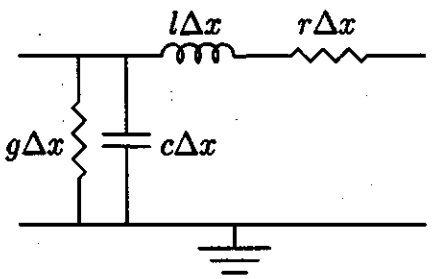

Figure 5.22 Distributed Model Section of a Transmission Line

length Δx together, the transmission line is formed.

For the case of a subscriber loop, the 2-wire pair causes the theoretical transmission line description to be further extended to show the parameters from line to line, as well as each line to ground, over the section Δx. This distributed model may be able to explain or better analyze the data collected in this thesis, but the extended analysis will be left for future research, as discussed in Section 6.3.

[10] See Section 2.1.2

5.3.2 Meter Measurement Results

To substantiate the capacitance measurements which were previously shown, tests were also conducted with a B+K Precision Universal LCR Meter. The 4075m line was measured again with faults of 98k, 22k, 12k, 6.8k, and 1.8kΩ at distances of 4075m, 2955m, and 1120m. The tip-ring capacitance results from these meter measurements are shown in Figures 5.23 and 5.24. The thick solid line shows the tip-ring capaci-

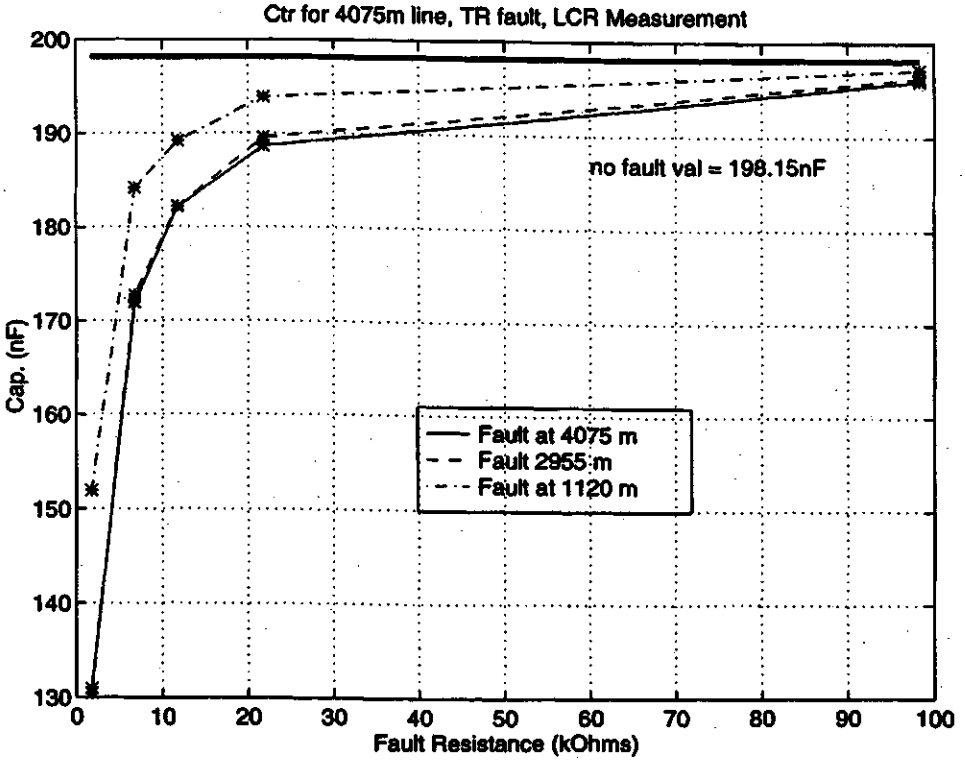

Figure 5.23 TR Capacitance for TR Fault, Measured by LCR Meter

tance with no faults on the line. Once again, the results are not a direct measurement, but are arrived at by solving a simple set of equations in MATLAB®, based on the equivalent circuit used for the loop analysis.

The results closely match the results taken with the DSP tester, shown in Figure 5.14 and 5.16, within approximately 4% (10nF). Since the error seems to be consistent throughout the data points, it can be attributed to either an offset in the

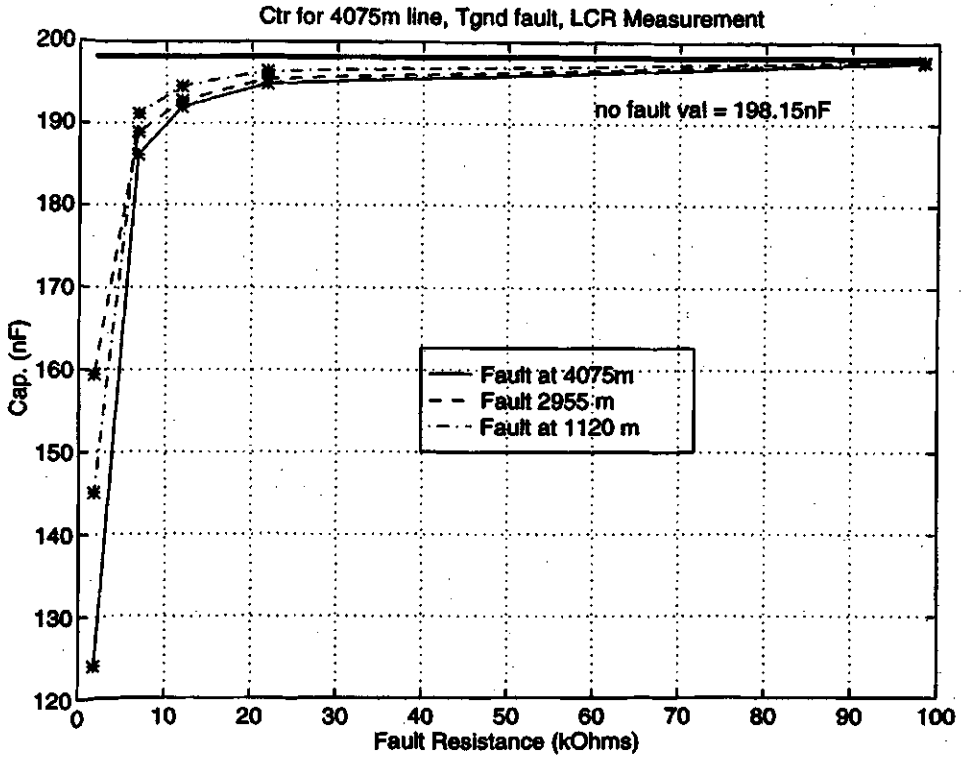

Figure 5.24 TR Capacitance for Tgnd Fault, Measured by LCR Meter

DSP-based tester, the LCR meter[11], or both. Since the DSP-based tester was tested for accuracy in Section 5.2, it is very possible that there is some contributing error in the LCR measurement. Although the results are slightly offset, the LCR measurement does help comfirm the shape of the DSP-tester results and the changes that are seen as fault parameters are varied.

5.3.3 Results Discussion

Although some of the results presented in this chapter are not intuitively as expected, the data does show correlation with various faults on the subscriber loop. Based on the type and resistance of the fault, as determined from the resistance measurements, the tip-ring capacitance plots can be used to roughly determine the location of the fault. By cross-referencing the known fault resistance on the bottom of the tip-ring capacitance plot with the measured tip-ring capacitance, an approximate estimate of the fault location can be determined.

For example, if a measured tip-ring resistance was found to be approximately 30kΩ, while the tip-ground and ring-ground resistances were 3MΩ or greater, then it can be assumed that a tip-ring fault of slightly less than 30kΩ has occured [12]. Assuming a 4075m loop and a measured tip-ring capacitance of 180nF, cross-referencing on Figure 5.14 would give an approximate distance of 3800m. Although the result may not be extremely accurate, it definitely gives a good idea of fault type and location.

Another example might assume a tip-ground fault, which would result in resistance measurements of 20kΩ between tip-ground and high impedance mesurements for tip-ring and ring-ground. If it is known that the loop being measured is 5005m long, then Figure 5.17 and 5.19 can be used to find the fault location given the tip-ring and/or tip-ground capacitance.

In order to make the fault analysis procedure more adaptable, the relationship between the capacitance measurements and the fault type and location is necessary.

[11]The LCR meter was not tested for accuracy prior to this test.

[12]Recall that the line accounts for a relatively small amount of the measured resistance.

Ideally, equations describing these relationships would allow the DSP-tester to conduct the analysis and report the fault summary, rather than the measured data. This analysis will be left for future work related to this project.

5.4 Summary

The results from testing done in Sections 5.1 and 5.2 have proven the capability of the DSP-based tester to make accurate measurements. When the tester was applied to a subscriber loop in Section 5.3, deviations could be seen in the line measurements as fault conditions changed and were moved. These deviations may be useful in trying to determine fault location and type.

6. CONCLUSION

6.1 Summary

The subscriber loop is an extremely important part of telephone networks. Although not considered the backbone, without the subscriber loop the end-user would not have access to the integrated world-wide communications network. Chapter 2 described some of the details of the network and examined a schematic representation of the subscriber loop. Some of the problems which can be encountered on the subscriber loop were discussed, including the effects of noise due to nearby power lines or other cables. The current test setup and measurement device was described and a table of measurement specifications was given.

Chapter 3 presented a high level system overview of the DSP-based subscriber loop tester. Hardware components were discussed, including the DSP chip itself, the TMS320C40. As described, the TMS320C40 and the ADC/DAC together provided ample sampling and processing power for the necessary task. Another part of the hardware system is the signal conditioning and switching, which was used as the interface between the ADC/DAC and the circuit/components under test. This description included a reference to the schematic diagram. Also in Chapter 3 was a summary of the software blocks which were responsible for making the proper measurements with the DSP chip and relaying the results and data back to the PC.

A detailed description of the measurement algorithms and the software implementation is described in Chapter 4. Measurement algorithms covered voltage (levels and frequency), resistance, and capacitance. Simulations were used to prove all algorithms before they could be trusted in the implementation. Also verified were post-data collection algorithms for analyzing the collected measurements.

The algorithms which were described in Chapter 4 were put to use in Chapter 5. The DSP-based tester was first used to measurement known voltages, resistances, and capacitances. Results were displayed in plots to show the accuracy of the measurements. Tests were then conducted on a twisted-pair of copper wire, which served as the subscriber loop in the lab environment. Various faults were created on the loop in order to understand the change in measured values. Results showed that changes in the fault resistance were linearly proportional to measured resistance values and also caused noticeable variations in measured capacitance.

6.2 Conclusions

The DSP-based subscriber loop tester appears to show results which may be helpful in determining the location and nature of faults on the subscriber loop. Initial measurements of voltages on the line would provide information which may lead to the cause of any problems and also protect service personnel which may be investigating the problem. Following a normal voltage test, resistance and capacitance measurements would be useful in finding a more inconspicuous problem. First, an abnormal resistance measurement would give insight into the fault resistance. This information can be used to cross- reference with the capacitance plot, which can be used to determine the approximate position of the fault [1].

From the nature of the results presented in Chapter 5, it can also be concluded that the line model used to analyze the data, including the calculation of parameters, may be suspect as a significant source of error for this project.

6.3 Future Research

Further analysis is needed to be able to deduce accurate fault information which would be useful in a commercial setting. Part of this work would involve extensive testing to accurately quantify the measurement results for various scenarios and represent these relationships in equation form. Along with this, it would be necessary

[1] In the case of a normal C_{tr}, this value can also be used to determine the length of the loop.

for the DSP loop tester to conclude fault analysis without external processing and make accurate recommendations for testing personnel to act upon. Also for future applications, more line data could be gathered by utilizing more of the processing power provided by the DSP chip on the tester. This may be helpful in analyzing subscriber loops for high-speed data capability and other possible uses.

As an alternative to continuing research utilizing the current state of the DSP-based subscriber loop tester, it may also be of interest to future reseachers to re-analyze the collected data using a distributed model line. Such a project may lead to results which can be more easily explained and therefore allow more accurate and detailed testing to follow.

References

[1] Morris et al., *Methods of and Apparatus for Determining the Capacitance of a Transmission Line by Integrating Line Currents*, US Patent 4320338, 1982.

[2] Masukawa et al., *Method and Apparatus of Measuring a Subscriber Line*, US Patent 5073920, 1991.

[3] Galloway et al., *Method and Apparatus for Analyzing Resistive Faults on Telephones Cables*, US Patent 5606592, 1997.

[4] Morgen, *Remote Testing of Telephone Loops*, US Patent 4054760, 1977.

[5] Shapiro, *Telephone Subscriber Line Fault Detector*, US Patent 5063585, 1991.

[6] Egozi, *Subscriber Line Impedance Measurement Device and Method*, US Patent 5465287, 1995.

[7] J. Bellamy, *Digital Telephony* (Second Edition), New York: John Wiley & Sons, 1991.

[8] Northern Telecom, *Lines Maintenance Guide*, BCS35 and up, Standard 01.03, December 1993.

[9] H.H. Skilling, *Electric Transmission Lines*, New York: McGraw-Hill Book Company Inc., 1951.

[10] Industry Canada, *Specification for Terminal Equipment, Terminal Systems, Network Protection Devices, Connection Arrangements and Hearing Aids Compatibility*, CS-03, Issue 8, June 1996, sec. 3.7.1.1.

[11] R.F. Tokarz, *TAD Seminars: Noise, Transmission, Inductive Interference* (Second Edition), Spokane, 1991.

[12] Northern Telecom, *Hardware Description Manual*, 297-8991-805, Standard 02.01, May 1995.

[13] Spectrum Signal Processing, *Quad C40 Processor Board - User's Guide*, Version 1.00, June 1993.

[14] Spectrum Signal Processing, *MDC40S TIM-40 Module - User's Manual*, Version 1.02, May 1993.

[15] Texas Instruments, *TMS320C4x User's Guide*, 1993.

[16] Texas Instruments, *TMS320C4x C Source Debugger*, 1992.

[17] Texas Instruments, *TMS320 Floating-Point DSP Optimizing C Compiler*, 1995.

[18] Spectrum Signal Processing, *Burr-Brown Analog Daughter Module - User Manual*, Version 1.04, August 1994.

[19] Spectrum Signal Processing, *PC Daughter Module Carrier Board - Technical Reference Manual*, Version 1.00, September 1992.

[20] R.E. Boucher and J.C. Hassab, "Analysis of Discrete Implementation of Generalized Cross Correlator", *IEEE Transactions on Acoustics, Speech, and Signal Processing*, Vol. 29, No. 3, June 1981, pp. 609-611.

[21] C. Daniel and F.S. Wood, *Fitting Equations to Data: Computer Analysis of Multifactor Data* (Second Edition), Toronto: John Wiley & Sons, 1980.

[22] A. Papoulis, *Probability, Random Variables, and Stochastic Processes* (Third Edition), New York: McGraw-Hill, Inc., 1991.

[23] W.D. Grover and D.E. Dodds, Course Notes for *EE589: Telecommunication Systems Engineering*, University of Alberta and University of Saskatchewan, 1996.

[24] J.A. Hill and P. Whelan, *Power Line Interference*, year unknown.

[25] The Mathworks Inc., *MATLAB ® - Reference Guide*, August 1992.

[26] J.G. Proakis and D.G. Manolakis, *Digital Signal Processing: Principles, Algorithms, and Applications* (Second Edition), New York: Macmillan Publishing Company, 1992.

A. APPENDIX A: Hardware Schematic

The schematic shown in Figure A.1 represents the interface circuit used for the DSP based subscriber loop tester. Inputs `DM1_CH0_OUT`, `DM2_CH0_OUT`, and `DM1_CH1_OUT` were used as control lines from the DAC to the components shown in the schematic. `DM1_CH0_IN` was the input to the ADC which sampled the desired signals.

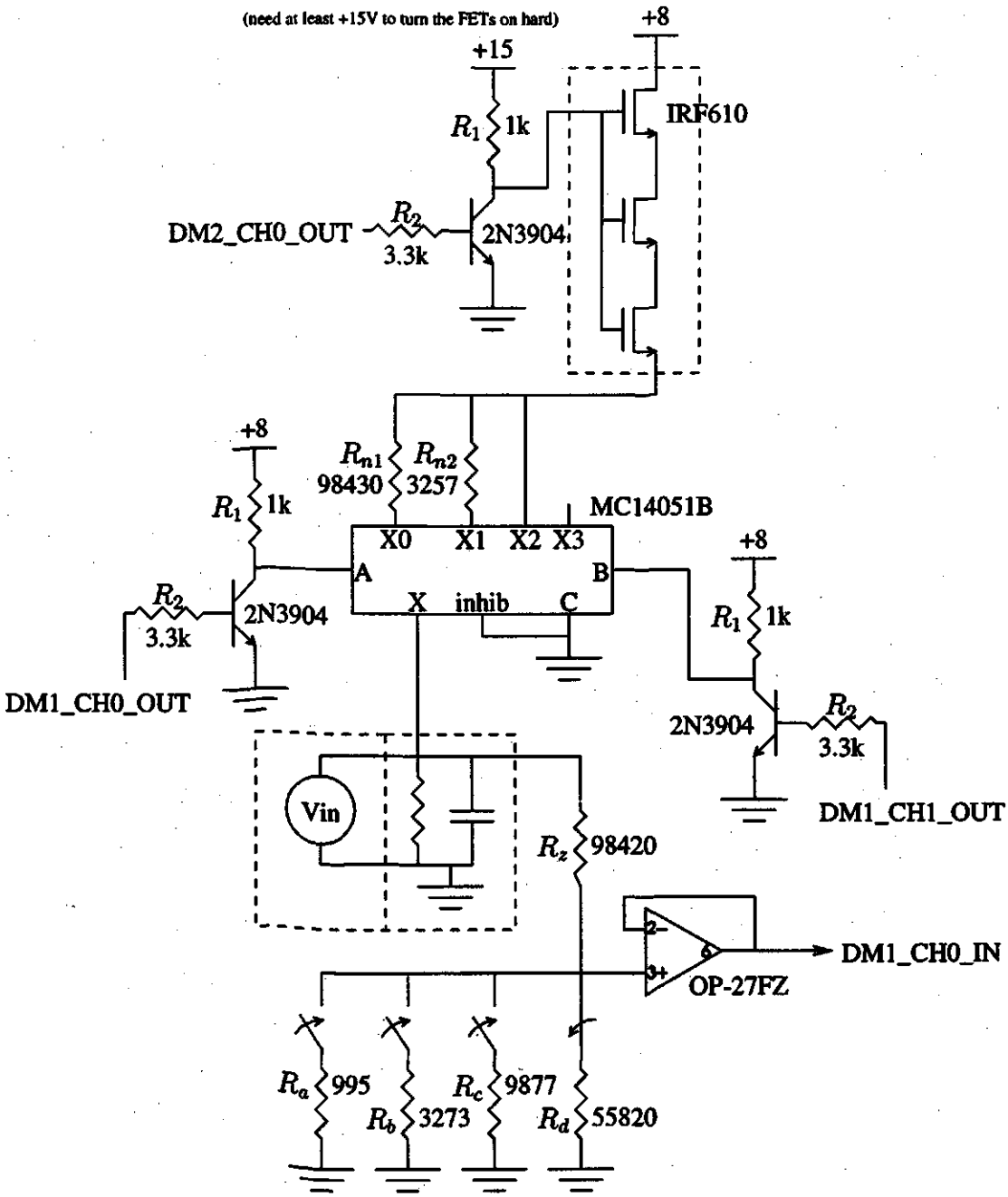

Figure A.1 Hardware Schematic

B. Appendix B: Tabulated Verification Results

The following tables list the measured results for known ac and dc input signals, as well as results for resistive and capacitive component measurements.

Table B.1 ac Voltage Measurements

Input Voltage (V)	Measured Voltage (V)				
0.010	0.010	0.009	0.009	0.010	0.010
0.100	0.100	0.100	0.100	0.100	0.100
0.250	0.248	0.248	0.249	0.249	0.249
0.500	0.499	0.499	0.499	0.499	0.499
1.000	0.999	0.999	0.999	0.999	0.999
2.000	1.987	1.989	1.989	1.989	1.990
3.000	2.991	2.990	2.989	2.991	2.991
4.000	3.991	3.991	3.990	3.990	3.993
5.000	4.989	4.987	4.986	4.987	4.989
6.000	5.974	5.972	5.973	5.971	5.973
7.000	6.978	6.973	6.974	6.974	6.973
8.000	7.977	7.974	7.972	7.971	7.973
ac voltages were measured at frequencies of 60, 103, 151, 199, 247 Hz					

Table B.2 dc Voltage Measurements

Input Voltage (V)	Measured Voltage (V)				
-8.001	-8.100	-8.100	-8.100	-8.100	-8.100
-7.000	-7.088	-7.088	-7.088	-7.087	-7.087
-6.000	-6.075	-6.075	-6.075	-6.075	-6.075
-5.000	-5.064	-5.064	-5.064	-5.064	-5.064
-4.000	-4.052	-4.052	-4.052	-4.052	-4.052
-3.000	-3.042	-3.042	-3.042	-3.041	-3.042
-1.999	-2.030	-2.029	-2.029	-2.029	-2.029
-1.000	-1.021	-1.021	-1.021	-1.020	-1.019
-0.500	-0.514	-0.514	-0.512	-0.513	-0.512
-0.249	-0.261	-0.261	-0.260	-0.260	-0.260
-0.100	-0.109	-0.109	-0.109	-0.109	-0.109
-0.010	-0.018	-0.017	-0.017	-0.017	-0.017
0.000	-0.007	-0.007	-0.007	-0.007	-0.007
0.010	0.003	0.003	0.003	0.003	0.003
0.100	0.094	0.094	0.094	0.094	0.094
0.248	0.247	0.246	0.246	0.246	0.246
0.500	0.501	0.500	0.500	0.500	0.500
0.998	1.005	1.004	1.003	1.003	1.003
2.002	2.020	2.019	2.019	2.018	2.018
3.001	3.030	3.028	3.028	3.028	3.028
4.001	4.038	4.038	4.038	4.038	4.038
4.999	5.048	5.047	5.047	5.047	5.047
6.001	6.062	6.061	6.061	6.061	6.061
7.002	7.074	7.074	7.074	7.074	7.074
8.002	8.085	8.085	8.084	8.084	8.084

Table B.3 Resistance & Capacitance Measurements for Various Resistance and 391.1nF & 99.3nF Capacitance

Resistance	391nF Cap		99.3nF Cap	
(kΩ)	Res (kΩ)	Cap (nF)	Res (kΩ)	Cap (nF)
2218	2075	388.2	2045	98.5
	2079	387.9	2047	98.5
	2079	375.4	2051	98.4
981	956	388.1	948	98.6
	957	375.8	949	98.6
	957	388.2	948	98.6
465	459	388.4	454	98.9
	459	388.5	454	98.9
	459	388.4	454	98.9
216	216	389.0	214	98.9
	216	388.9	214	98.9
	216	388.8	214	98.8
98	98	389.5	98	98.8
	98	389.2	98	98.8
	98	389.1	98	98.8
56	56	389.8	56	99.2
	56	389.8	56	99.1
	56	389.7	56	99.1
11.8	11.80	390.7	11.77	100.4
	11.80	390.6	11.77	100.4
	11.80	390.6	11.77	100.4
1.792	1.876	363.3	1.873	98.9
	1.876	363.5	1.874	98.8
	1.876	363.1	1.873	98.8

Table B.4 Resistance & Capacitance Measurements for Various Resistance and 55.5nF & 15.15nF Capacitance

Resistance	55.5nF Cap		15.15nF Cap	
(kΩ)	Res (kΩ)	Cap (nF)	Res (kΩ)	Cap (nF)
2218	2067	55.0	2026	14.7
	2068	55.0	2025	14.8
	2069	55.0	2023	14.8
981	955	55.0	953	14.7
	956	55.0	954	14.7
	954	55.0	954	14.7
465	458	55.0	458	14.8
	459	55.0	459	14.8
	459	55.0	459	14.8
216	216	55.1	216	14.8
	216	55.1	216	14.8
	216	55.1	216	14.8
98	98	55.3	99	14.9
	98	55.3	99	14.9
	98	55.3	99	14.9
56	56	55.4	56	15.1
	56	55.4	56	15.1
	56	55.4	56	15.1
11.8	11.76	56.8	11.80	16.2
	11.76	56.8	11.79	16.2
	11.76	56.8	11.79	16.3
1.792	1.873	60.0	1.875	tf
	1.874	60.4	1.875	tf
	1.874	54.0	1.875	tf

tf: too fast of a decay to get at least 5 samples at 75 kHz

C. Appendix C: Tabulated Loop Results

The tables in Appendix C list the values from the measurements which were conducted on the subscriber loop. Data is shown for the 5005m and 4075m lengths, with both TR and Tgnd faults. The listed values are the raw data and must be processed by the equations described in Section 4.4 to find the loop parameters shown in Figure 2.3.

Table C.1 Subscriber Loop Measurements for 5005m Line, TR Fault

Condition	Parameter	No Faults				
Tip grounded	Res	2999	2999	2999	2999	2999
	Cap	235.5	235.4	235.5	234.5	235.2
Ring grounded	Res	2999	2999	2999	2999	2999
	Cap	234.5	235.2	235.3	234.6	234.6
TR shorted	Res	2999	2999	2999	2999	2999
	Cap	0.6	0.7	0.7	0.7	0.6
		100kΩ TR short @ 5005m				
Tip grounded	Res	97	97	97	97	97
	Cap	240.0	239.9	240.7	240.6	240.0
Ring grounded	Res	97	97	97	97	97
	Cap	240.0	239.9	240.5	239.9	239.9
TR shorted	Res	2999	2999	2999	2999	2999
	Cap	0.6	0.7	0.7	0.7	0.7
		22kΩ TR short @ 5005m				
Tip grounded	Res	22.95	22.94	22.95	22.95	22.95
	Cap	228.9	228.8	227.0	228.7	227.1
Ring grounded	Res	22.95	22.95	22.95	22.95	22.95
	Cap	228.7	228.9	226.9	229.0	227.2
TR shorted	Res	2999	2999	2999	2999	2999
	Cap	0.7	0.7	0.6	0.6	0.6

Resistances in kΩ, Capacitances in nF

Condition	Parameter	12kΩ TR short @ 5005m				
Tip grounded	Res	13.07	13.07	13.07	13.07	13.07
	Cap	216.4	216.4	218.9	216.2	218.8
Ring grounded	Res	13.07	13.07	13.07	13.07	13.07
	Cap	218.8	218.9	216.4	216.5	219.0
TR shorted	Res	2999	2999	2999	2999	2999
	Cap	0.7	0.6	0.7	0.6	0.7
		6.8kΩ TR short @ 5005m				
Tip grounded	Res	8.065	8.064	8.064	8.064	8.063
	Cap	202.4	202.6	202.5	205.9	202.6
Ring grounded	Res	8.064	8.063	8.064	8.063	8.065
	Cap	202.6	202.4	205.8	202.5	202.3
TR shorted	Res	2999	2999	2999	2999	2999
	Cap	0.6	0.7	0.6	0.7	0.6
		1.8kΩ TR short @ 5005m				
Tip grounded	Res	3.270	3.269	3.270	3.269	3.269
	Cap	146.9	143.2	143.3	146.9	143.2
Ring grounded	Res	3.270	3.270	3.270	3.270	3.270
	Cap	143.2	146.9	146.8	143.2	143.2
TR shorted	Res	2999	2999	2999	2999	2999
	Cap	0.7	0.6	0.7	0.7	0.7
		100kΩ TR short @ 3575m				
Tip grounded	Res	97	97	97	97	97
	Cap	240.1	240.9	240.1	240.2	240.2
Ring grounded	Res	97	97	97	97	97
	Cap	240.8	240.3	240.3	240.1	240.1
TR shorted	Res	2999	2999	2999	2999	2999
	Cap	1.1	1.1	1.1	1.1	1.0
Resistances in kΩ, Capacitances in nF						

Condition	Parameter	22kΩ TR short @ 3575m				
Tip	Res	22.60	22.60	22.60	22.60	22.60
grounded	Cap	228.0	228.1	229.8	229.8	229.9
Ring	Res	22.60	22.60	22.60	22.60	22.60
grounded	Cap	229.7	227.9	228.1	227.9	229.9
TR	Res	2999	2999	2999	2999	2999
shorted	Cap	1.1	1.1	1.0	1.1	1.0
		12kΩ TR short @ 3575m				
Tip	Res	12.71	12.71	12.71	12.71	12.71
grounded	Cap	220.4	217.2	220.4	217.8	220.4
Ring	Res	12.71	12.71	12.71	12.71	12.71
grounded	Cap	220.2	217.3	220.4	220.2	220.4
TR	Res	2999	2999	2999	2999	2999
shorted	Cap	1.0	1.1	1.1	1.0	1.0
		6.8kΩ TR short @ 3575m				
Tip	Res	7.695	7.696	7.695	7.695	7.695
grounded	Cap	206.9	207.0	203.3	207.0	206.9
Ring	Res	7.695	7.695	7.695	7.695	7.696
grounded	Cap	207.0	207.1	203.4	206.9	207.0
TR	Res	2999	2999	2999	2999	2999
shorted	Cap	1.1	1.1	1.1	1.0	1.0
		1.8kΩ TR short @ 3575m				
Tip	Res	2.879	2.879	2.879	2.879	2.879
grounded	Cap	139.7	139.7	139.7	139.7	139.7
Ring	Res	2.879	2.879	2.879	2.879	2.879
grounded	Cap	139.7	139.7	139.7	139.7	139.7
TR	Res	2999	2999	2999	2999	2999
shorted	Cap	1.1	1.1	1.1	1.1	1.1
Resistances in kΩ, Capacitances in nF						

Condition	Parameter	100kΩ TR short @ 2145m				
Tip grounded	Res	97	97	97	97	97
	Cap	241.7	241.6	241.7	241.8	240.9
Ring grounded	Res	97	97	97	97	97
	Cap	240.9	240.8	241.7	240.8	241.7
TR shorted	Res	2999	2999	2999	2999	2999
	Cap	1.1	1.1	1.0	1.1	1.1
		22kΩ TR short @ 2145m				
Tip grounded	Res	22.22	22.22	22.22	22.22	22.23
	Cap	233.0	231.0	231.1	233.1	233.0
Ring grounded	Res	22.22	22.23	22.22	22.22	22.23
	Cap	231.2	232.8	231.3	233.1	233.2
TR shorted	Res	2999	2999	2999	2999	2999
	Cap	1.1	1.0	1.0	1.1	1.0
		12kΩ TR short @ 2145m				
Tip grounded	Res	12.32	12.32	12.33	12.33	12.32
	Cap	222.5	225.8	225.6	222.4	222.5
Ring grounded	Res	12.32	12.32	12.32	12.32	12.32
	Cap	225.9	222.5	225.8	222.7	222.7
TR shorted	Res	2999	2999	2999	2999	2999
	Cap	1.0	1.1	1.0	1.1	1.1
		6.8kΩ TR short @ 2145m				
Tip grounded	Res	7.310	7.311	7.310	7.311	7.310
	Cap	215.1	215.3	215.2	211.1	215.2
Ring grounded	Res	7.311	7.310	7.310	7.311	7.311
	Cap	211.0	211.0	211.0	210.9	215.2
TR shorted	Res	2999	2999	2999	2999	2999
	Cap	1.1	1.0	1.1	1.1	1.1
Resistances in kΩ, Capacitances in nF						

Condition	Parameter	1.8kΩ TR short @ 2145m				
Tip grounded	Res	2.477	2.478	2.477	2.478	2.478
	Cap	149.7	149.7	149.7	149.7	149.7
Ring grounded	Res	2.478	2.478	2.478	2.477	2.478
	Cap	149.7	149.7	149.7	149.7	149.7
TR shorted	Res	2999	2999	2999	2999	2999
	Cap	1.1	1.1	1.1	1.1	1.1
		100kΩ TR short @ 715m				
Tip grounded	Res	96	96	96	96	96
	Cap	242.5	243.2	242.4	243.1	243.1
Ring grounded	Res	96	96	96	96	96
	Cap	243.0	242.4	242.5	242.3	243.1
TR shorted	Res	2999	2999	2999	2999	2999
	Cap	1.0	1.1	1.0	1.1	1.1
		22kΩ TR short @ 715m				
Tip grounded	Res	21.83	21.83	21.83	21.84	21.83
	Cap	236.8	237.1	236.9	238.7	237.2
Ring grounded	Res	21.83	21.83	21.84	21.83	21.83
	Cap	238.7	239.0	236.8	237.2	237.0
TR shorted	Res	2999	2999	2999	2999	2999
	Cap	1.0	1.0	1.0	1.1	1.1
		12kΩ TR short @ 715m				
Tip grounded	Res	11.94	11.94	11.94	11.94	11.94
	Cap	233.0	236.0	232.9	236.1	233.0
Ring grounded	Res	11.94	11.94	11.94	11.94	11.94
	Cap	235.7	236.0	232.9	235.9	232.7
TR shorted	Res	2999	2999	2999	2999	2999
	Cap	1.1	1.0	1.1	1.1	1.1

Resistances in kΩ, Capacitances in nF

Condition	Parameter	6.8kΩ TR short @ 715m				
Tip grounded	Res	7.362	7.362	7.363	7.363	7.362
	Cap	218.4	218.4	213.8	218.3	218.5
Ring grounded	Res	7.363	7.362	7.363	7.363	7.362
	Cap	218.4	213.7	218.3	213.8	218.4
TR shorted	Res	2999	2999	2999	2999	2999
	Cap	1.1	1.1	1.0	1.1	1.1
		1.8kΩ TR short @ 715m				
Tip grounded	Res	2.075	2.075	2.075	2.075	2.075
	Cap	187.0	187.1	187.1	187.1	187.1
Ring grounded	Res	2.075	2.075	2.075	2.075	2.075
	Cap	187.0	187.1	187.1	187.1	187.1
TR shorted	Res	2999	2999	2999	2999	2999
	Cap	1.0	1.0	1.0	1.0	1.1
Resistances in kΩ, Capacitances in nF						

Table C.2 Subscriber Loop Measurements for 5005m Line, Tgnd Fault

Condition	Parameter	100kΩ Tgnd @ 5005m				
Tip grounded	Res	2999	2999	2999	2999	2999
	Cap	235.5	235.0	234.7	235.0	235.3
Ring grounded	Res	97	97	97	97	97
	Cap	238.7	239.0	236.8	237.2	237.0
TR shorted	Res	99	99	99	99	99
	Cap	1.2	1.2	1.2	1.2	1.2
		22kΩ Tgnd @ 5005m				
Tip grounded	Res	2999	2999	2999	2999	2999
	Cap	235.1	234.9	234.8	234.7	235.5
Ring grounded	Res	22.31	22.31	22.31	22.31	22.31
	Cap	233.4	235.6	235.3	235.6	233.6
TR shorted	Res	22.42	22.42	22.42	22.42	22.42
	Cap	1.9	1.9	1.9	1.9	1.9
		12kΩ Tgnd @ 5005m				
Tip grounded	Res	2999	2999	2999	2999	2999
	Cap	234.9	235.8	235.1	235.8	235.6
Ring grounded	Res	12.40	12.40	12.40	12.40	12.40
	Cap	226.8	229.5	229.6	229.8	229.6
TR shorted	Res	12.45	12.45	12.45	12.45	12.45
	Cap	tf	tf	tf	tf	tf

Resistances in kΩ, Capacitances in nF
tf: decay was too fast to be measured

Condition	Parameter	6.8kΩ Tgnd @ 5005m				
Tip grounded	Res	2999	2999	2999	2999	2999
	Cap	235.1	235.0	235.6	235.8	235.9
Ring grounded	Res	7.398	7.398	7.398	7.398	7.398
	Cap	217.6	217.6	222.1	222.1	217.8
TR shorted	Res	7.410	7.410	7.410	7.410	7.410
	Cap	tf	tf	tf	tf	tf
		1.8kΩ Tgnd @ 5005m				
Tip grounded	Res	2999	2999	2999	2999	2999
	Cap	236.0	235.6	235.4	235.8	235.6
Ring grounded	Res	2.574	2.574	2.574	2.574	2.574
	Cap	162.6	162.9	162.6	162.7	162.7
TR shorted	Res	2.574	2.574	2.574	2.574	2.574
	Cap	tf	tf	tf	tf	tf
		100kΩ Tgnd @ 3575m				
Tip grounded	Res	2999	2999	2999	2999	2999
	Cap	234.8	235.1	235.0	235.6	235.6
Ring grounded	Res	96	96	96	96	96
	Cap	242.2	243.0	242.9	242.9	242.1
TR shorted	Res	98	98	98	98	98
	Cap	1.2	1.2	1.2	1.2	1.2
		22kΩ Tgnd @ 3575m				
Tip grounded	Res	2621	2596	2592	2590	2586
	Cap	236.5	235.7	236.7	236.4	236.0
Ring grounded	Res	21.97	21.98	21.97	21.97	21.98
	Cap	236.5	236.6	236.4	236.5	236.3
TR shorted	Res	22.09	22.09	22.08	22.08	22.08
	Cap	1.9	1.9	1.9	1.9	1.9

Resistances in kΩ, Capacitances in nF
tf: decay was too fast to be measured

Condition	Parameter	12kΩ Tgnd @ 3575m				
Tip grounded	Res	2596	2595	2591	2613	2589
	Cap	236.1	236.4	236.0	236.2	236.8
Ring grounded	Res	12.16	12.16	12.16	12.16	12.16
	Cap	231.0	228.0	228.2	231.0	228.1
TR shorted	Res	12.19	12.19	12.19	12.19	12.19
	Cap	tf	tf	tf	tf	tf
		6.8kΩ Tgnd @ 3575m				
Tip grounded	Res	2486	2509	2489	2487	2487
	Cap	236.9	236.6	236.3	236.8	236.1
Ring grounded	Res	7.168	7.168	7.168	7.167	7.167
	Cap	218.4	218.4	223.1	223.2	223.2
TR shorted	Res	7.179	7.178	7.178	7.179	7.179
	Cap	tf	tf	tf	tf	tf
		1.8kΩ Tgnd @ 3575m				
Tip grounded	Res	2480	2480	2481	2484	2481
	Cap	237.1	236.5	236.9	236.5	237.0
Ring grounded	Res	2.360	2.360	2.360	2.360	2.360
	Cap	161.8	161.9	161.7	161.8	161.9
TR shorted	Res	2.360	2.360	2.360	2.360	2.360
	Cap	tf	tf	tf	tf	tf
		100kΩ Tgnd @ 2145m				
Tip grounded	Res	2479	2477	2476	2497	2477
	Cap	236.2	236.8	237.1	236.2	237.0
Ring grounded	Res	95	95	95	95	95
	Cap	243.5	244.2	243.4	243.6	243.4
TR shorted	Res	97	97	97	97	97
	Cap	1.2	1.2	1.2	1.2	1.2

Resistances in kΩ, Capacitances in nF
tf: decay was too fast to be measured

Condition	Parameter	22kΩ Tgnd @ 2145m				
Tip grounded	Res	2471	2469	2467	2486	2466
	Cap	236.9	236.1	236.1	236.0	236.7
Ring grounded	Res	21.75	21.75	21.75	21.75	21.75
	Cap	236.6	236.8	236.8	238.6	236.8
TR shorted	Res	21.86	21.86	21.86	21.86	21.86
	Cap	1.9	1.9	1.9	1.9	1.9
		12kΩ Tgnd @ 2145m				
Tip grounded	Res	2477	2478	2477	2478	2478
	Cap	236.7	237.1	236.1	236.1	236.3
Ring grounded	Res	11.96	11.95	11.95	11.95	11.95
	Cap	234.2	231.4	231.7	234.3	231.3
TR shorted	Res	11.98	11.98	11.98	11.98	11.98
	Cap	tf	tf	tf	tf	tf
		6.8kΩ Tgnd @ 2145m				
Tip grounded	Res	2477	2478	2479	2479	2479
	Cap	236.0	236.9	236.1	236.3	236.2
Ring grounded	Res	7.378	7.378	7.378	7.378	7.378
	Cap	215.9	215.9	211.8	211.8	211.3
TR shorted	Res	7.382	7.383	7.382	7.382	7.381
	Cap	tf	tf	tf	tf	tf
		1.8kΩ Tgnd @ 2145m				
Tip grounded	Res	2478	2476	2492	2471	2470
	Cap	236.4	237.2	236.8	237.1	236.9
Ring grounded	Res	2.162	2.162	2.162	2.162	2.162
	Cap	169.4	169.2	169.2	169.2	169.0
TR shorted	Res	2.162	2.162	2.162	2.162	2.162
	Cap	tf	tf	tf	tf	tf

Resistances in kΩ, Capacitances in nF
tf: decay was too fast to be measured

Condition	Parameter	100kΩ Tgnd @ 715m				
Tip grounded	Res	2500	2478	2501	2481	2482
	Cap	236.9	236.8	235.8	236.2	236.3
Ring grounded	Res	95	95	95	95	95
	Cap	244.9	244.1	244.0	244.9	244.9
TR shorted	Res	97	97	97	97	97
	Cap	tf	tf	tf	tf	tf
		22kΩ Tgnd @ 715m				
Tip grounded	Res	2474	2497	2477	2475	2475
	Cap	236.7	235.9	236.7	236.2	237.0
Ring grounded	Res	21.56	21.56	21.56	21.56	21.56
	Cap	241.3	241.4	239.3	241.4	239.3
TR shorted	Res	21.67	21.67	21.67	21.67	21.67
	Cap	1.9	1.9	1.9	1.9	1.9
		12kΩ Tgnd @ 715m				
Tip grounded	Res	2476	2479	2475	2498	2477
	Cap	237.0	235.9	236.3	236.3	236.0
Ring grounded	Res	11.76	11.76	11.76	11.76	11.76
	Cap	239.7	239.4	236.2	239.6	236.6
TR shorted	Res	11.79	11.79	11.80	11.80	11.80
	Cap	tf	tf	tf	tf	tf
		6.8kΩ Tgnd @ 715m				
Tip grounded	Res	2471	2468	2487	2465	2466
	Cap	236.7	237.0	236.8	237.0	236.1
Ring grounded	Res	7.181	7.181	7.181	7.181	7.181
	Cap	225.0	225.4	225.2	219.6	225.0
TR shorted	Res	7.186	7.187	7.186	7.186	7.186
	Cap	tf	tf	tf	tf	tf

Resistances in kΩ, Capacitances in nF
tf: decay was too fast to be measured

Condition	Parameter	1.8kΩ Tgnd @ 715m				
Tip grounded	Res	2488	2466	2464	2482	2459
	Cap	236.9	236.8	236.8	236.9	236.4
Ring grounded	Res	1.963	1.963	1.962	1.962	1.962
	Cap	190.8	191.0	190.8	190.9	191.3
TR shorted	Res	1.963	1.963	1.963	1.963	1.963
	Cap	tf	tf	tf	tf	tf

Resistances in kΩ, Capacitances in nF
tf: decay was too fast to be measured

Table C.3 Subscriber Loop Measurements for 4075m Line, TR Fault

Condition	Parameter	No Faults				
Tip grounded	Res	2999	2999	2999	2999	2999
	Cap	190.9	191.6	191.0	191.3	190.8
Ring grounded	Res	2999	2999	2999	2999	2999
	Cap	190.8	191.2	191.2	190.9	190.8
TR shorted	Res	2999	2999	2999	2999	2999
	Cap	1.1	1.1	1.1	1.1	1.1
		100kΩ TR @ 4075m				
Tip grounded	Res	98	98	98	98	98
	Cap	193.6	193.5	194.1	193.8	193.9
Ring grounded	Res	98	98	98	98	98
	Cap	194.1	193.7	193.5	193.6	193.8
TR shorted	Res	2999	2999	2999	2999	2999
	Cap	1.1	1.1	1.1	1.1	1.1
		22kΩ TR @ 4075m				
Tip grounded	Res	22.75	22.75	22.75	22.75	22.75
	Cap	185.0	185.8	185.4	185.0	185.3
Ring grounded	Res	22.75	22.75	22.75	22.75	22.75
	Cap	186.1	185.8	185.9	185.2	185.1
TR shorted	Res	2999	2999	2999	2999	2999
	Cap	1.1	1.1	1.1	1.1	1.1
		12kΩ TR @ 4075m				
Tip grounded	Res	12.84	12.84	12.84	12.84	12.84
	Cap	178.3	179.7	179.6	179.5	179.5
Ring grounded	Res	12.84	12.84	12.84	12.84	12.84
	Cap	179.7	178.3	179.6	179.6	179.6
TR shorted	Res	2999	2999	2999	2999	2999
	Cap	0.7	0.7	0.7	0.7	0.7
Resistances in kΩ, Capacitances in nF						

Condition	Parameter	6.8kΩ TR @ 4075m				
Tip grounded	Res	7.822	7.822	7.822	7.822	7.824
	Cap	168.9	168.8	168.9	168.8	170.6
Ring grounded	Res	7.821	7.823	7.822	7.823	7.822
	Cap	168.8	168.8	169.0	168.9	170.8
TR shorted	Res	2999	2999	2999	2999	2999
	Cap	1.1	1.1	1.1	1.1	1.1
		1.8kΩ TR @ 4075m				
Tip grounded	Res	3.016	3.016	3.016	3.016	3.016
	Cap	123.6	123.6	123.6	123.7	123.6
Ring grounded	Res	3.016	3.016	3.016	3.016	3.016
	Cap	123.6	123.6	123.6	123.7	123.7
TR shorted	Res	2999	2999	2999	2999	2999
	Cap	1.1	1.1	1.1	1.1	1.1
		100kΩ TR @ 2955m				
Tip grounded	Res	97	97	97	97	97
	Cap	193.8	193.8	193.7	193.7	193.7
Ring grounded	Res	97	97	97	97	97
	Cap	194.1	194.2	194.2	193.9	193.7
TR shorted	Res	2999	2999	2999	2999	2999
	Cap	0.7	1.1	1.0	1.0	1.1
		22kΩ TR @ 2955m				
Tip grounded	Res	22.45	22.45	22.46	22.46	22.45
	Cap	186.0	186.9	186.6	185.9	186.7
Ring grounded	Res	22.46	22.46	22.46	22.46	22.46
	Cap	186.5	186.9	185.5	186.4	185.7
TR shorted	Res	2999	2999	2999	2999	2999
	Cap	1.1	1.0	1.1	1.1	1.0
Resistances in kΩ, Capacitances in nF						

Condition	Parameter	12kΩ TR @ 2955m				
Tip grounded	Res	12.55	12.55	12.55	12.55	12.55
	Cap	180.5	178.9	180.5	180.4	180.5
Ring grounded	Res	12.55	12.55	12.55	12.55	12.55
	Cap	180.6	180.4	179.3	179.2	180.3
TR shorted	Res	2999	2999	2999	2999	2999
	Cap	1.1	1.1	1.0	1.1	1.1
		6.8kΩ TR @ 2955m				
Tip grounded	Res	7.531	7.531	7.531	7.532	7.531
	Cap	171.8	172.0	170.1	169.8	172.0
Ring grounded	Res	7.532	7.532	7.532	7.532	7.532
	Cap	172.0	171.8	171.8	171.8	170.0
TR shorted	Res	2999	2999	2999	2999	2999
	Cap	1.0	1.1	1.0	1.0	1.1
		1.8kΩ TR @ 2955m				
Tip grounded	Res	2.703	2.703	2.703	2.703	2.703
	Cap	122.0	122.0	122.0	122.0	122.0
Ring grounded	Res	2.703	2.703	2.703	2.703	2.703
	Cap	122.0	122.0	122.0	122.0	122.1
TR shorted	Res	2999	2999	2999	2999	2999
	Cap	1.0	1.1	1.0	1.0	1.1
		100kΩ TR @ 1120m				
Tip grounded	Res	97	97	97	97	97
	Cap	195.3	195.2	194.8	194.8	194.7
Ring grounded	Res	97	97	97	97	97
	Cap	194.4	194.4	195.2	195.0	194.8
TR shorted	Res	2999	2999	2999	2999	2999
	Cap	0.8	0.7	0.7	0.7	0.7

Resistances in kΩ, Capacitances in nF

Condition	Parameter	22kΩ TR @ 1120m				
Tip grounded	Res	21.96	21.96	21.96	21.96	21.96
	Cap	190.0	190.6	189.4	190.2	190.2
Ring grounded	Res	21.96	21.96	21.96	21.96	21.96
	Cap	189.8	190.1	189.5	190.7	191.0
TR shorted	Res	2999	2999	2999	2999	2999
	Cap	0.7	0.7	0.8	0.8	0.7
		12kΩ TR @ 1120m				
Tip grounded	Res	12.05	12.05	12.05	12.05	12.05
	Cap	185.9	185.5	187.1	185.5	187.4
Ring grounded	Res	12.05	12.05	12.05	12.05	12.05
	Cap	185.4	187.1	185.8	185.5	185.4
TR shorted	Res	2999	2999	2999	2999	2999
	Cap	0.7	0.8	0.7	0.8	0.7
		6.8kΩ TR @ 1120m				
Tip grounded	Res	7.015	7.013	7.013	7.013	7.013
	Cap	180.7	183.1	180.3	182.8	183.1
Ring grounded	Res	7.014	7.013	7.013	7.013	7.013
	Cap	183.1	183.0	180.7	183.1	180.4
TR shorted	Res	2999	2999	2999	2999	2999
	Cap	0.8	0.8	0.8	0.7	0.7
		1.8kΩ TR @ 1120m				
Tip grounded	Res	2.177	2.177	2.177	2.177	2.177
	Cap	142.1	142.0	142.1	142.1	142.0
Ring grounded	Res	2.177	2.177	2.177	2.177	2.177
	Cap	142.1	142.0	142.1	142.0	142.0
TR shorted	Res	2999	2999	2999	2999	2999
	Cap	0.7	0.7	0.7	0.7	0.7

Resistances in kΩ, Capacitances in nF

Table C.4 Subscriber Loop Measurements for 4075m Line, Tgnd Fault

Condition	Parameter	100kΩ Tgnd @ 4075m				
Tip grounded	Res	2999	2999	2999	2999	2999
	Cap	191.6	191.3	191.0	191.3	191.3
Ring grounded	Res	97	97	97	97	97
	Cap	194.9	194.5	194.8	195.2	194.7
TR shorted	Res	99	99	99	99	99
	Cap	1.2	1.2	1.2	1.2	1.2
		22kΩ Tgnd @ 4075m				
Tip grounded	Res	2999	2999	2999	2999	2999
	Cap	191.1	191.0	191.2	191.1	190.8
Ring grounded	Res	22.20	22.20	22.20	22.20	22.20
	Cap	188.4	190.1	189.4	189.4	189.1
TR shorted	Res	22.29	22.30	22.30	22.30	22.30
	Cap	2.0	2.0	2.0	2.0	2.0
		12kΩ Tgnd @ 4075m				
Tip grounded	Res	2999	2999	2999	2999	2999
	Cap	191.6	191.6	191.5	190.9	191.3
Ring grounded	Res	12.30	12.30	12.30	12.30	12.30
	Cap	182.8	183.6	183.3	184.4	182.9
TR shorted	Res	12.33	12.33	12.33	12.33	12.33
	Cap	tf	tf	tf	tf	tf
		6.8kΩ Tgnd @ 4075m				
Tip grounded	Res	2999	2999	2999	2999	2999
	Cap	190.8	191.2	191.2	191.6	191.2
Ring grounded	Res	7.282	7.280	7.281	7.281	7.281
	Cap	176.0	174.2	177.0	176.2	174.0
TR shorted	Res	7.293	7.294	7.294	7.293	7.293
	Cap	tf	tf	tf	tf	tf

Resistances in kΩ, Capacitances in nF
tf: decay was too fast to be measured

Condition	Parameter	1.8kΩ Tgnd @ 4075m				
Tip grounded	Res	2999	2999	2999	2999	2999
	Cap	191.5	191.0	191.3	190.9	190.7
Ring grounded	Res	2.444	2.444	2.444	2.444	2.444
	Cap	111.2	111.3	111.1	111.8	111.0
TR shorted	Res	2.444	2.444	2.444	2.444	2.444
	Cap	tf	tf	tf	tf	tf
		100kΩ Tgnd @ 2955m				
Tip grounded	Res	2999	2999	2999	2999	2999
	Cap	191.4	191.2	191.1	190.9	191.1
Ring grounded	Res	97	97	97	97	97
	Cap	195.1	194.5	195.1	195.1	195.2
TR shorted	Res	99	99	99	99	99
	Cap	1.1	1.2	1.1	1.2	1.2
		22kΩ Tgnd @ 2955m				
Tip grounded	Res	2999	2999	2999	2999	2999
	Cap	191.6	191.5	191.2	191.3	191.6
Ring grounded	Res	22.07	22.07	22.07	22.07	22.07
	Cap	187.2	189.5	188.7	187.6	187.5
TR shorted	Res	22.16	22.16	22.15	22.16	22.16
	Cap	1.9	1.9	1.9	1.9	1.9
		12kΩ Tgnd @ 2955m				
Tip grounded	Res	2999	2999	2999	2999	2999
	Cap	191.3	191.3	191.4	191.6	191.7
Ring grounded	Res	12.15	12.16	12.15	12.15	12.15
	Cap	179.5	181.3	181.1	182.2	179.7
TR shorted	Res	12.18	12.18	12.18	12.18	12.18
	Cap	tf	tf	tf	tf	tf

Resistances in kΩ, Capacitances in nF
tf: decay was too fast to be measured

Condition	Parameter	6.8kΩ Tgnd @ 2955m				
Tip grounded	Res	2999	2999	2999	2999	2999
	Cap	191.7	191.0	191.3	191.8	191.9
Ring grounded	Res	7.140	7.141	7.141	7.140	7.139
	Cap	165.4	166.9	165.8	167.6	164.2
TR shorted	Res	7.147	7.149	7.146	7.145	7.148
	Cap	tf	tf	tf	tf	tf
		1.8kΩ Tgnd @ 2955m				
Tip grounded	Res	2999	2999	2999	2999	2999
	Cap	191.8	191.5	190.5	190.7	190.5
Ring grounded	Res	2.289	2.289	2.289	2.289	2.289
	Cap	98.2	98.5	98.2	97.9	98.2
TR shorted	Res	2.289	2.289	2.289	2.289	2.289
	Cap	tf	tf	tf	tf	tf
		100kΩ Tgnd @ 1120m				
Tip grounded	Res	2999	2999	2999	2999	2999
	Cap	191.0	191.8	191.2	192.1	191.0
Ring grounded	Res	96	96	96	96	96
	Cap	195.4	195.3	195.6	195.7	195.6
TR shorted	Res	98	98	98	98	98
	Cap	0.9	0.9	0.9	0.9	0.9
		22kΩ Tgnd @ 1120m				
Tip grounded	Res	2999	2999	2999	2999	2999
	Cap	191.6	191.9	191.2	191.4	191.9
Ring grounded	Res	21.78	21.78	21.78	21.78	21.78
	Cap	191.6	191.1	192.7	192.2	193.1
TR shorted	Res	21.88	21.87	21.88	21.88	21.88
	Cap	tf	tf	tf	tf	tf

Resistances in kΩ, Capacitances in nF
tf: decay was too fast to be measured

Condition	Parameter	12kΩ Tgnd @ 1120m				
Tip grounded	Res	2999	2999	2999	2999	2999
	Cap	192.1	191.4	190.9	192.1	191.7
Ring grounded	Res	11.90	11.89	11.89	11.89	11.89
	Cap	190.1	188.9	189.0	190.6	190.0
TR shorted	Res	11.92	11.92	11.92	11.92	11.92
	Cap	tf	tf	tf	tf	tf
		6.8kΩ Tgnd @ 1120m				
Tip grounded	Res	2999	2999	2999	2999	2999
	Cap	191.2	191.7	191.2	191.4	191.6
Ring grounded	Res	7.303	7.304	7.304	7.304	7.303
	Cap	174.4	173.6	176.3	173.8	173.9
TR shorted	Res	7.307	7.307	7.308	7.307	7.308
	Cap	tf	tf	tf	tf	tf
		1.8kΩ Tgnd @ 1120m				
Tip grounded	Res	2999	2999	2999	2999	2999
	Cap	191.3	191.7	191.2	191.5	192.4
Ring grounded	Res	2.027	2.027	2.027	2.027	2.027
	Cap	127.3	127.5	127.5	127.3	126.9
TR shorted	Res	2.027	2.027	2.027	2.027	2.027
	Cap	tf	tf	tf	tf	tf

Resistances in kΩ, Capacitances in nF
tf: decay was too fast to be measured